Development of Recombinant Human Collagen Type I and Type III Injectable Hydrogels for Cardiac Therapy.

By:
James Podrebarac

This thesis is submitted as a partial fulfillment of the M.Sc. program in Cellular and Molecular Medicine

Supervisors: Erik Suuronen and Emilio Alarcon

Department of Cellular and Molecular Medicine
Faculty of Medicine
University of Ottawa
Ottawa, Ontario, Canada

Abstract

Functional biomaterials are being developed as scaffolds to support endogenous cells and to promote the regeneration of ischemic tissue. The aim for this study was to develop a new translational platform for injectable hydrogels using recombinant human collagen (rHC) of two types: type I (TI) and type III (TIII). The collagen solutions were characterized to ensure batch-to-batch consistency and protein integrity. The hydrogel preparation protocol was extensively monitored to ensure ease of use and high-quality production. Post-gelation, rHC TIII have a higher viscosity compared to rHC TI, yet water content was high for both hydrogels. The cross-linking degree is similar for both rHC hydrogels, which are stable well above physiological temperatures, but rHC TI is more susceptible to enzymatic degradation than rHC TIII. Furthermore, the micro-architecture differed with pore size dimensions of rHC TIII being significantly larger than that of rHC TI. Cardiac fibroblasts were cultured on the rHC hydrogels, and cells attached readily to the scaffold environment, which promoted proliferation. The rHC matrices mechanical and biological properties provide structural support, and demonstrate biodegradability and biocompatibility. The intrinsic physical differences between the rHC hydrogels will likely have implications in future studies. In conclusion, the rHC TI and TIII hydrogels are proven to be suitable matrices for continued investigation towards future translational applications.

Table of Contents

Abstract ..... **ii**

Table of Contents ..... **iii**

List of Tables ..... **iv**

List of Illustrations ..... **v**

List of Abbreviations ..... **vi**

Acknowledgements ..... **vii**

1 Chapter: Introduction **1**

1.1 Regenerative Medicine in Cardiovascular Disease 1
1.2 Functional Biomaterials: Natural, Synthetic, and Novel Scaffolds 4
1.3 Collagen-based Matrices for Cardiac Therapy 9
1.4 Biomaterials in Cardiac Translational Medicine 13
1.5 Rationale and Project Objectives 17

2 Chapter: Materials and Methods **19**

2.1 Collagen Solution Consistency and Stability for Hydrogel Use 19
2.2 Collagen Hydrogel Production and Physical Analysis 22
2.3 Evaluation of the Collagen Hydrogels with Cardiac Relevant Cells 28

3 Chapter: Results **32**

3.1 Characterization of Collagen Solutions 32
3.2 Optimization of the Collagen Hydrogel Protocol 33
3.3 Characterization of Collagen Hydrogels 37
3.4 Biocompatibility of Collagen Hydrogels 44

4 Chapter: Discussion **51**

4.1 Significance and Interpretations 51
4.2 Future Directions 67

5 Chapter: Conclusion **70**

Bibliography **71**

List of Tables

Table 3-1: Physical properties of Theracol, rHC TI, and rHC TIII solutions prior to hydrogels production 33

Table 3-2: Overview for production of Theracol, rHC TI, and rHC TIII hydrogels using the t-piece mixing system..... 35

Table 3-3: Overview of the modifications to the hydrogel production protocol 36

Table 3-4: Final stepwise overview for the production of Theracol, rHC TI, and rHC TIII hydrogels using the t-piece mixing system..... 35

List of Illustrations

Figure 2-1: Schematic of t-piece system hydrogel preparation 24

Figure 3-1: Maximum viscosity of hydrogels..... 38

Figure 3-2: Water content of hydrogels..... 39

Figure 3-3: Denaturation temperature of hydrogels 40

Figure 3-4: Enzymatic degradation of hydrogels in collagenase..... 41

Figure 3-5: Detection of chemical cross-linker by-product release from hydrogels 43

Figure 3-6: Select cryo-SEM images of the micro-architecture for hydrogels..... 45

Figure 3-7: Pore size dimensions for hydrogels 46

Figure 3-8: Morphology of cardiac fibroblasts cultured on rHC hydrogels 47

Figure 3-9: Immunohistochemistry composite images of cardiac fibroblasts seeded on rHC hydrogels..... 48

Figure 3-10: Cardiac fibroblast proliferation after culture on rHC hydrogels..... 49

List of Abbreviations

CVD	cardiovascular disease
HF	heart failure
LV	left ventricular
MI	myocardial infarction
ECM	extracellular matrix
TERM	tissue engineering / regenerative medicine
GF	growth factor
PCL	poly(DL-lactide-co-caprolaone)
PLGA	poly(DL-lactide-co-glycolide
PLA	poly(lactic acid)
RGD	fibronectin tripeptide (Arg-Gly-Asp)
YIGSR	laminin pentapeptide (Tyr-Ile-Gly-Ser-Arg)
VEGF	vascular endothelial growth factor
MMP	matrix metalloproteinase
MSC	mesenchymal stem cell
rHC TI	recombinant human collagen type I
rHC TIII	recombinant human collagen type III
SOP	standard operating procedure
CD	circular dichroism
PBS	phosphate buffer saline
CS-C	chondroitin sulphate-C
MES	2-morpholinoethane sulfonic acid monohydrate
EDC	N-(3-dimethylaminopropyl)-N'-ethylcarbodiimide
NHS	N-hydroxysuccinimide
NaOH	sodium hydroxide
DSC	differential scanning calorimetry
cryo-SEM	low temperature scanning electron microscopy
HBSS	Hank's balanced salt solution
DMEM	Dulbecco’s modified eagle medium
TCPS	tissue culture polystyrene
DAPI	4',6-diamidino-2-phenylindole
WGA-488	wheat germ agglutinin 488

Acknowledgements

I sincerely thank Dr. Erik Suuronen and Dr. Emilio Alarcon for their encouragement and leadership. I have learned so much under your supervision. I am always amazed by your insight and expertise. I am very grateful for all the assistance from Brian McNeill, Branka Vulesevic, Donna Padavan, Nick Blackburn, and Suzanne Crowe throughout the project. Sarah McLaughlin, I believe your commitment to our parallel projects truly represents the virtues of a cohesive scientific team.

Furthermore, I thank my committee members: Dr. Marc Ruel and Dr. Qiao Li for their valuable support and feedback. I appreciate the academic accommodations granted by the University of Ottawa Heart Institute, and I am thankful for my funding sources: Alexander Graham Bell Canada Graduate Scholarship (CGS-M/NSERC) and Ontario Graduate Scholarship (OGS).

In addition, I thank my friends who have shown me their support time and time again: G.B., O.C., R.D., R.P., A.C., and Xuro – you guys are the best. J.B. – keep doing your dailies, bless up. M.A. – One Punch Manuel! Thanks for all the laughs. H.B. – one coffee sip and bottle of wine at a time. S.M. – the cells will grow, the gels will work, and the sectioning will end... soon?

I extend my deepest gratitude to my mother and father. Their patience, love, and motivation have guided me throughout not only my graduate studies, but the entirety of my life. I also thank my brother, Ricky, for his uplifting humour and attention to my concerns. Finally, I am appreciative of your love, Natascha Ramos. Your support has always given me the drive to move forward.

1 Chapter: Introduction

1.1 Regenerative Medicine in Cardiovascular Disease

Cardiovascular disease (CVD) is recognized as an assortment of adverse conditions that damage the cardiovascular system leading to loss of function or failure (Georgiadis et al., 2014, Hilfiker-Klemer, 2006). In consideration of the ageing population and long-term unhealthy lifestyles, the acute and chronic impact of CVD on individuals, families, and healthcare institutions is enormous. CVD remains one of the leading causes of death worldwide, even though its prevalence has declined in the last decade (Mozaffarian et al., 2014). Heart failure (HF), the result of hypertrophy and left ventricular (LV) remodeling of cardiac tissue, occurs after acute trauma by myocardial infarction (MI) or the progression of hypertension, atherosclerosis or cardiomyopathies (Epelman et al., 2015, Hilfiker-Klemer, 2006).

In MI, the narrowing of coronary arteries initially restricts blood flow to the heart, which deprives resident cardiomyocytes of oxygen (hypoxia) and nutrients resulting in massive cell death in the LV area (Epelman et al., 2015, Frangogiannis, 2014). Consequently, this ischemic tissue undergoes remodeling and develops a fibrotic scar. This adverse remodeling and loss of cardiomyocyte mass results in structural and functional limitations in heart contractility and its ability to pump blood (Vilahur et al., 2011, Distefano and Sciacca, 2012). The highly differentiated tissue of the myocardium is vulnerable to injury, lacking an extensive, dynamic repair and regenerative capacity post-MI (Steinhauser and Lee, 2011). Cardiac remodeling corresponds to infarct expansion, ventricular dilation and ventricular wall stresses that affect patient morbidity and mortality. Although surgical procedures and pharmacological (*i.e.* vasodilators,

diuretics) treatments can minimize cardiac dysfunction, the improvement is temporary for some patients and only circumvents the complication (Chachques et al., 2013, Distefano and Sciacca, 2012). Ultimately, end-stage HF patients undergo heart transplantation or high-risk patients are implanted with ventricular assist devices with intensive drug therapy (Georgiadis et al., 2014, Steinhauser and Lee, 2011). The post-MI scar represents a target for developing treatments that may repair and regenerate ischemic tissues in patients.

The initiation and propagation of adverse remodeling due to ischemic injury are modulated by immune and extracellular matrix (ECM) molecular signals (Epelman et al., 2015, Vilahur et al., 2011). Importantly, the evolution of the infarct is categorized by three distinct stages: inflammatory phase, proliferative phase, and maturation phase (Epelman et al., 2015, Frangogiannis, 2014). In the heart, acute inflammation post-MI is cardioprotective in the presence of short-term, intensive stress (Frangogiannis, 2014, Shen et al., 2013). Cellular necrosis and ECM degradation during tissue injury release pro-inflammatory signals, which increases infiltration of neutrophils and macrophages (Epelman et al., 2015, Frangogiannis, 2014, Shen et al., 2013). Subsequently, in the proliferative phase, myofibroblast proliferation promotes infarct stabilization by the release of ECM reparative signals and scar tissue formation (Epelman et al., 2015). Nonetheless, post-MI inflammation is propelled by reperfusion that establishes an intensive pro-inflammatory environment. Currently, no exact molecular mechanism(s) has thoroughly explained MI and post-MI inflammation involved in ischemic injury. Furthermore, autocrine and paracrine interactions accelerate myocardial responses to stress and injury (Zhang et al., 2015b, Steinhauser and Lee, 2011). These phenomena are

good focal points for elucidating a means to understand and manipulate cardiac regenerative functions. However, it is clear that inflammation, severe loss of myocyte mass, and fibrosis contribute to adverse remodeling (Epelman et al., 2015, Vilahur et al., 2011). One approach to restore the structural and functional integrity of the heart is to prevent or reverse the hostile environment and adverse remodeling.

Cardiac stem cell therapies are considered important for the future of cardiac regeneration treatments. It is now confirmed that the adult heart has intrinsic regeneration capabilities, specifically induced by differentiating cardiomyocytes, endogenous progenitors, and bone marrow sources (Steinhauser and Lee, 2011, Garbern and Lee, 2013). However, this regeneration is quite limited by the small myocyte turnover rate over decades in adult life (Steinhauser and Lee, 2011, Garbern and Lee, 2013). Nonetheless, this information has lead to new technologies that involve the delivery of stem cells to ischemic or infarcted cardiac tissue (Garbern and Lee, 2013). Cells with intrinsic progenitor/repair functions are considered for therapies such as bone-marrow-derived stem cells, embryonic stem cells, cardiac stem cells, or inducible pluripotent stem cells (Garbern and Lee, 2013, Schussler et al., 2010, Segers and Lee, 2008). Overall, the regenerative treatments intend to restore blood flow and/or cardiomyocyte mass in localized scarred tissues, particularly LV remodeling, and improve cardiac function (Garbern and Lee, 2013, Schussler et al., 2010, Murry et al., 2006).

Cell-based therapies have shown great potential in laboratory trials, yet the results in clinical trials have been less impressive and inconsistent. Direct injection of cells, although most common in therapies, have many limitations such as poor engraftment, efficacy, and low survival (Sanganalmath and Bolli, 2013, Ye et al., 2011, Schussler et

al., 2010, Suuronen et al., 2008). Furthermore, there are issues with appropriate cell-type choice, cell transplantation timing, and delivery technique (Sanganalmath and Bolli, 2013, Kuraitis et al., 2010, Murry et al., 2006). The limitations in cell-based therapies are also associated with a general lack of knowledge in cardiac regeneration. Although there is evidence for two theories on the source of cardiomyocyte replenishment in adults, whether from stem and progenitor cells or mature cardiomyocytes, it is unclear which mechanism is most prevalent and how the regenerative process changes post-MI (Garbern and Lee, 2013, Steinhauser and Lee, 2011). Furthermore, as stated above, missing information involving fundamental processes that influence the ischemic environment and adverse remodeling impede therapeutic advancement in this new field. In order to improve on the successes of cell therapy and cardiac regeneration, new complementary approaches are necessary.

1.2 Functional Biomaterials: Natural, Synthetic, and Novel Scaffolds

The advancement in engineered functional biomaterials for cardiac therapies may be promising for addressing the demands of CVD worldwide. Biomaterials are natural or synthetic 3-dimensional scaffolds that are designed to mimic and interact with the local cellular microenvironment (Tallawi et al., 2015, Lam and Wu, 2012, Rane and Christman, 2011). The field of tissue engineering/regenerative medicine (TERM) focuses on restoring structural and functional properties in damaged tissues (Shapira et al., 2016, Tallawi et al., 2015). For cardiovascular applications, biomaterials are intended to support or temporarily replace defective myocardial tissue whilst providing a template for long-term repair or regeneration. For example, biomaterials aim to accomplish this task

by regulating cellular and molecular mechanisms (*i.e.* inflammation, fibrosis), enhancing ECM and tissue integrity, and promoting cardiomyocyte viability and regeneration (Finosh and Jayabalan, 2012, Segers and Lee, 2011, Kuraitis et al., 2010). In order to adhere to TERM criteria, biomaterials must display mechanical and biological features that are biocompatible, biodegradable, and biomimetic (Boffito et al., 2014, Rane and Christman, 2011). Currently, biomaterial approaches for therapeutic efficacy involve *in-vivo* / *ex-vivo* cell seeding onto implantable scaffolds or acellular scaffolds that recruit endogenous cells to facilitate reparative processes (Tallawi et al., 2015, Boffito et al., 2014). Biomaterial scaffolds can be used to deliver cells to designated regions, whilst improving engraftment and survivability (Schussler et al., 2010, Suuronen et al., 2008). They can be combined with various cytokines or growth factors (GFs) that are known to promote angiogenesis or neovascularization in cardiac tissues (Shapira et al., 2016, Tallawi et al., 2015). Scaffold structural and mechanical properties, including anisotropic and topographic cues, can modulate cardiomyocyte and fibroblast morphology, distribution, and function similarly to the healthy myocardial environment (Silvestri et al., 2013, Wang et al., 2011, Schussler et al., 2010). The scope of the endeavour is broad, and as such there are numerous differences in material preparation, composition, and modification (Boffito et al., 2014, Rane and Christman, 2011). These materials are usually prepared as cardiac patches, fibrous sheets, macroporous sponges and foams, or hydrogels (see below) with differences in shape and size (Shapira et al., 2016, Asti and Gioglio, 2014). Furthermore, these qualities dictate material physical, mechanical, and biological properties. Thus, it is crucial that biomaterials are characterized in comparison to the environment (ECM, myocardial tissue) intended for their use.

Natural-based scaffolds, comprised of polysaccharides and/or proteins, can be designed to have characteristics that mimic physical and biological features of the native heart ECM (Shapira et al., 2016). These materials are frequently made with collagen (see below), fibrin, alginate, chitosan, and hyaluronic acid (Zhang et al., 2015b, Asti and Gioglio, 2014). In general, these components are biocompatible and bioactive, based on natural origin, that promote cell adhesion, proliferation, and differentiation (Rane and Christman, 2011). Decellularized tissues, undergoing thorough pre- and post-processing, maintain tissue-specific features important for material-host interactions with multi-layered biological networks that have non-cellular components intact (Londono and Badylak, 2015, Galvez-Monton et al., 2013). This scaffold embodies the biological micro-architecture of the complex, native ECM in the heart (Johnson and Christman, 2013). However, factors such as cost, poor stability and reproducibility, and relatively weak mechanical properties present a common problem to natural scaffolds (Shapira et al., 2016, Hasan et al., 2015, Zhang et al., 2015b). Furthermore, immunogenicity may be an issue for clinical translation due to the risks involved in preparation (contamination) and origin (animal-based) of the biomaterial (Shapira et al., 2016).

Synthetic scaffolds lack intrinsic biocompatible features but have greater versatility in design and preparation. Typically, polyesters and polyurethanes are used for consistent, inexpensive production with readily customizable and precise physical and mechanical properties (Shapira et al., 2016, Zhang et al., 2015b). Furthermore, some synthetics are biodegradable, such as polycaprolactone (PCL), poly(lactic-co-glycolic acid) (PLGA), and poly(lactic acid) (PLA), and most are easily modifiable (Asti and Gioglio, 2014, Galvez-Monton et al., 2013). Though advantageous in design, drawbacks

include foreign body response, toxicity, and undefined functional interaction (Silvestri et al., 2013). In addition, synthetics typically have surface hydrophobicity and lack internal or external biological components, without modification, that hinder cultivating interactions for cell growth and tissue organization (Asti and Gioglio, 2014).

Hybrid biomaterials combine natural and synthetic aspects in design choice to produce superior structural and functional properties in scaffolds (Silvestri et al., 2013, Lam and Wu, 2012). Hybrid production methods tend to be multi-faceted, involving many different techniques (*e.g.* gas foaming, freeze drying, electrospinning) to assemble a unified scaffold (Boffito et al., 2014). Typically, natural components are layered over synthetic components, whether as multi-layered fibers or shell and core constructs. Synthetics reinforce mechanical properties or impart unique geometries to the scaffold while natural components modify exterior biointegration and surface interactions (D'Amore et al., 2016). Markedly, compartmentalized or whole material geometry (*e.g.* shape, size, porosity, fiber dimensions) influence cell alignment, permeation and contractility movements. This is commonly displayed with electrospun fibrous scaffolds (Prabhakaran et al., 2012, Heydarkhan-Hagvall et al., 2008) or self-assembling peptides (Martinez-Ramos et al., 2014). However, composite or hybrid biomaterials require extensive characterization to ensure the individual properties imparted by each component are maintained throughout pre- and post- processing methods.

Biomaterials can undergo morphological, chemical, and biological modifications to enhance their structural or functional properties. These modifications are implemented during material production (*e.g.* cross-linking, bioactive molecules) or after production (*e.g.* surface functionalization). For example, cell adhesion may be improved with

specific functional groups or cell-binding motifs (RGD, YIGSR) used on surface coatings (Tallawi et al., 2015, Zhang et al., 2015b). Laser embedded micro-channels, which improve cell attachment and retention, can physically alter scaffold surfaces with precision (Muehleder et al., 2014). GFs, such as vascular endothelial growth factor (VEGF) or insulin-like growth factor 1, can stimulate regenerative processes in cardiac tissues (Shapira et al., 2016). GFs can be linked to scaffolds by means of covalent fixation to surfaces, encapsulation, or cross-linkage (Shapira et al., 2016, Lee et al., 2011). Composite scaffolds, particularly hydrogels, readily expose GFs to tissues by specific localization and degradation controlled time-release (Lee et al., 2011). These modifications can improve cell survival and mediate growth, proliferation, and differentiation (Rane and Christman, 2011).

Injectable hydrogels, natural or synthetic, are hydrated solutions that are designed to solidify in response to physiological pH, temperature, and chemical cross-linking (Johnson and Christman, 2013, Ye et al., 2011, McEwan et al., 2011). Hydrogels are soft materials, which form complex, hydrophilic 3D environments that are highly water absorbent, malleable, and robust (Hasan et al., 2015). The high water retention and polymeric network, often enhanced by covalent cross-linkage, is appropriate for environmental biomimetic applications (Hasan et al., 2015, Ye et al., 2011). Hydrogels offer surface adhesion and permeability, maximized by the structural expansion with water retention and porous networks. This facilitates cellular interactions with the material, providing physical and functional support. In addition, the spatial organization of solidified hydrogels act as a scaffold improving the retention and function of transplanted cells (Johnson and Christman, 2013). Furthermore, *in situ* gelation is an

advantageous property of hydrogels because as an injectable the delivery system minimizes invasive procedures and delivers easily compared to rigid materials such as tissue patches or delicate decellularized sheets (Johnson and Christman, 2013, Wang et al., 2010). Interestingly, injectable materials have the ability, without administration of exogenous cells, to improve cardiac function and minimize LV dilation in animal models (Johnson and Christman, 2013, Christman et al., 2004). The mechanisms involved in the material-cell-host interactions that promote functional regeneration and tissue neovascularization have not been fully elucidated. Indeed, structural support provided by an inert material has little to no significant impact alone (Johnson and Christman, 2013). Therefore, investigational focus should emphasize the most clinically viable materials and their bioactive interactions in the cardiac environment.

1.3 Collagen-based Matrices for Cardiac Therapy

In particular, collagen receives a lot of attention as a capable natural scaffold for tissue engineering. The class of fibrous structural protein collagens, in fibrillar and non-fibrillar forms, are found in most mammalian connective tissues comprising about 25% of total dry weight (Parenteau-Bareil et al., 2010). Collagens are uniquely characterized by a triple helical domain, formed by the assembly of three polypeptide α-chains with repeating Gly-X-Y sequences into a homotrimeric or heterotrimeric supramolecular structure (Parenteau-Bareil et al., 2010, Caulfield and Janicki, 1997). The repeated triplet sequence has glycine residues at every third position followed by hydroxylysine, hydroxyproline, or proline residues in the X and Y positions (Chattopadhyay and Raines, 2014, Parenteau-Bareil et al., 2010, Engel and Prockop, 1991). This particular sequence

allows for coiled turns in the polypeptide chains. The structural properties differ between collagen types, associated to differences in α-chain composition, but the helical formation remains conserved in fibrillar collagens (Chattopadhyay and Raines, 2014, Engel and Prockop, 1991). Primarily, collagens are prepared and secreted (as procollagen) from fibroblasts undergoing post-translational modifications. Externally, the tropocollagen self-assembly produces fibrils that build towards collagen fibers (Chattopadhyay and Raines, 2014, Parenteau-Bareil et al., 2010). Furthermore, the fibrillar collagens type I - (90%; $[\alpha1(I)]_2\alpha2(I)$) and type III - (10%; $[\alpha1(III)]_3$) are major components in the ECM of cardiac tissue (Shapira et al., 2016, Parenteau-Bareil et al., 2010, Caulfield and Janicki, 1997). The majority of fibers surrounding cardiomyocytes are co-polymerized type I and type III bundles (Gazoti Debessa et al., 2001). Importantly, these collagens provide structural and functional support to the surrounding cardiac tissues and are organized in three distinct layers/bundles: epimysial, perimysial, and endomysial fibers (Shapira et al., 2016). The organization of these collagen networks, specific alignment and orientation of fibers, provides a functional surface for cellular growth, communication, and contractility (Shapira et al., 2016, Haneef et al., 2012). Furthermore, collagen motifs (*e.g.* RGD) interact with numerous cell receptor (*e.g.* integrins) proteins and other components of the ECM (Chattopadhyay and Raines, 2014, Parenteau-Bareil et al., 2010). These direct and indirect interactions provide cellular cues for adhesion, migration, proliferation, and differentiation (Chattopadhyay and Raines, 2014, Parenteau-Bareil et al., 2010). Intrinsically, collagens have excellent biocompatibility and biodegradability characteristics. Both type I and type III collagens are abundant, integral components to healthy cardiac ECM structure and function. Furthermore, collagen biodegradation is

natively regulated by matrix metalloproteinases (MMPs; collagenases) enzymatic activity. In developing collagen-based biomaterials, these properties can be modulated by cross-linking techniques (physical, chemical, and enzymatic) that form polymeric networks (Davidenko et al., 2015, Delgado et al., 2015, Parenteau-Bareil et al., 2010). Although these properties make collagen advantageous for biomaterial purposes, there are also a few drawbacks. Its mechanical properties are quite conserved making optimization difficult and unmodified polymers have poor conduction. As well, cautious handling is necessary to avoid denaturation, degradation, or fibrillogenesis.

Importantly, the two major types of ECM collagen, type I and type III, have significantly different structures (Pauschinger et al., 1999, Marijianowski et al., 1995). This impacts their role and mechanical features in the native heart ECM. Collagen type I is the most abundant, providing strength and stiffness that establishes the fibrous networks whereas collagen type III modulates myocyte function and is inter-dispersed in collagen type I networks providing elasticity (Tallawi et al., 2015, Pauschinger et al., 1999). It is known that the ECM ratio between these collagen influences the physical and mechanical properties of the native and post-MI tissues (Wei et al., 1999). Generally, type I is heightened compared to type III in diseased hearts (Caulfield and Janicki, 1997) whereas early-stage post-MI type III increases significantly resulting in reduced adhesion and angiogenesis (Schussler et al., 2010). This ratio-dependent phenomenon is considered in other pathological conditions, such as vascular Ehlers-Danlos syndrome, and influences fibril covalent cross-linking differences between the two collagens (Liu et al., 1997, Henkel and Glanville, 1982). In ageing, collagen type I content increases and myocyte numbers decrease with the development of new fibers at the LV wall (Gazoti

Debessa et al., 2001). This is similar to ratio differences over time in uninjured and hypertrophic skin. Relatedly, the type I/III ratio is altered with less elastic type III that may denote loss of cardiac function. It is known that type I fibrillogenesis, that is fiber growth and length/diameter, is influenced by type III during co-assembly in the cardiac environment (Liu et al., 1997). Furthermore, an increased collagen type I/III ratio in myocardial fibrosis is associated with dilated cardiomyopathy (Pauschinger et al., 1999). These differences in myocardial collagen type I/III disposition at varying stages of life or injury can possibly influence the impact of collagen-based materials.

Collagen-based scaffolds, predominately with collagen type I, have been a staple natural source for cardiac biomaterials. In our lab, collagen-based matrices have improved vascularization and repair of ischemic and infarcted tissues (Blackburn et al., 2015, Ahmadi et al., 2014, Kuraitis et al., 2012a). It is apparent that collagen materials go beyond simplistic structural support roles. Collagen materials are highly suitable for GF delivery. Studies show that the controlled degradation of collagen materials can increase GF retention and concurrent angiogenesis (Shapira et al., 2016, Tabata et al., 2000). Alternatively, collagen matrices are compatible cell delivery or recruitment materials that improve cell transplantation and retention with tissue-specificity (Ahmadi et al., 2014, Mayfield et al., 2014, Zhang et al., 2008). Collagen, as an appropriate regenerative environment, provides biophysical and biochemical cues that regulate cell behaviour (Gasiorowski et al., 2013). In particular, collagen supports the cellular growth and functionality of many stem cells and progenitors such as circulating angiogenic cells, mesenchymal stem cells (MSCs), and skeletal myoblasts (Kuraitis et al., 2012b, Wang et al., 2010, Dai et al., 2009). In addition, some methods promote stem cell differentiation

into cardiomyocytes with pre-conditioned collagen scaffolds for cardiac phenotypes, such as scaffold electrostimulation (Nunes et al., 2013, Haneef et al., 2012) or decellularized hybrid materials (Duan et al., 2011). Collagen hydrogels or soft-matrices exhibit these positive cellular interactions best, attributed to their 3D environments (Hasan et al., 2015, Segers and Lee, 2011).

While collagen alone is a desirable natural choice for composite scaffolds, it can be supplemented with additional components, such as polysaccharides (Deng et al., 2010) or other ECM-derived proteins (Pieper et al., 2000, Cao and Xu, 2008) for improved function. Scaffolds comprised of synthetic materials such as PCL, PLGA, and PLA benefit from collagen for cell attachment and differentiation (Liu et al., 2016, Prabhakaran et al., 2014, Park et al., 2005). In recent nano-material approaches, collagen nanofibers infused with gold nanoparticles were able to enhance fiber conductivity and promote MSC differentiation in cardiac differentiation medium (Orza et al., 2011). The mechanical and biological properties that collagen biomaterials offer are ideal for cardiac regeneration. Furthermore, the range of pre- and post-production modifications allows collagen to advance with novel design methods, nanotechnology, and composites that are at the forefront of next-generation materials.

1.4 Biomaterials in Cardiac Translational Medicine

Although progress in the field has been admirable, TERM biomaterials for cardiovascular treatments are not yet widely ready for the clinic. This is apparent by the lack of ongoing clinical trials over the last few years. Certification of approval from medical authorities for material implantation trials, especially with stem cells, is a strictly

regulated and arduous process. Important to risk-to-benefit ratio assessment, proof of efficacy and long-term safety are mandatory requirements in approval. Biomechanical and functional performance of biomaterials differs considerably depending on preparation, composition, and modification. Therefore, it is difficult to balance material biologic performance with structural stability (degradation rates, mechanical properties) for cardiac applications (Vunjak-Novakovic et al., 2010). This is increasingly important for TERM requirements involving cardiac vascularization, electrostimulation, and ECM integration (Chachques et al., 2013, Finosh and Jayabalan, 2012). In terms of safety, scaffolds must display biocompatibility, biodegradability, and biointegration without local and systemic immunogenic, teratogenic, and toxic consequences (Ogle et al., 2016, Finosh and Jayabalan, 2012). This is most problematic with animal-derived or synthetic components, and notably a hindrance for stem cell populations. Furthermore, scaffolds intended for clinical purposes should demonstrate potential for scale-up methods, accessible transference techniques, and shelf life duration. In addition, stem cells incorporated into scaffolds require comprehensive documentation of cell and scaffold preparation, manufacturing, and biological potency that must adhere to regulations associated with each component. For current cardiac tissue engineering an ideal biomaterial has yet to address all these major challenges, which impede clinical progression. Predominately, material applications that are currently approved for human use are heart valve replacements, endovascular stents, and various vascular grafts (Lam and Wu, 2012). Nonetheless, current breakthroughs with novel methods (*e.g.* nanotechnologies, bio-printing, hybrid materials, injectables, functionalization) are beginning to overcome these problems. Less than a decade ago, the MAGNUM trial

(Myocardial Assistance by Grafting a New Bioartificial Upgraded Myocardium - nonrandomized, controlled phase I) was the first clinical biomaterial trial for infarct repair (Chachques et al., 2008). A collagen matrix implant with bone marrow cells was grafted onto the infarct scar. The treatment was safe and the results were positive, yet small sample size limited the significance. Recently, the PRESERVATION I trial (IK-5001 for the Prevention of Remodeling of the Ventricle and Congestive Heart Failure After Acute Myocardial Infarction - multicenter, randomized, double-blind, placebo-controlled phase I/II) advanced the field with an injectable bioabsorbable alginate matrix that cross-links into a biological scaffold (Rao et al., 2016, Rao et al., 2015). The intracoronary injectable material aimed to mediate adverse remodeling 2 to 5 days after successful reperfusion in patients. Unfortunately, though safe and feasible, the material failed to elicit positive changes to LV remodeling or cardiac events over 6 months (Rao et al., 2016). International initiatives for cardiac TERM biomaterials, such as the RECATABI Project (Regeneration of Cardiac Tissue Assisted by Bioactive Implants), will help build upon this foundation for novel, translational biomaterials (Soler-Botija et al., 2014, Galvez-Monton et al., 2013). The objective for RECATABI was the development of new bioengineered scaffolds that transport and protect stem cells for ischemic tissue restoration. The project outcome devised two elastomeric microporous materials with self-assembly nanofiber hydrogels: a non-degradable polyethylacrylate membrane and semi-degradable caprolactone 2-(methacryloyloxy)ethyl ester membrane (Chachques et al., 2013).

Tissue engineered scaffolds are increasingly popular as *in-vitro* proof-of-concept studies, which elaborate on new properties and techniques. However, these studies fail to

consider translational aspects and may not be followed up by *in-vivo* characterization. Furthermore, *in-vivo* projects require larger sample sizes, longer time-point experiments and a transition from small to large animals to fully understand potential therapeutic impact (Ogle et al., 2016). In this direction, knowledge on material-cell-host interactions and the mechanisms that drive improvements in cardiac function and remodeling will be necessary (Johnson and Christman, 2013, Finosh and Jayabalan, 2012). To a degree, positive outcomes are likely dependent on personalized conditions such as infarct size, inflammatory progression, and physiological adaptation (*e.g.* gender, age, condition). Furthermore, scaffold mechanical properties must resist movement in the dynamic environment of the heart, such as hemodynamic forces and muscle contractility (Vunjak-Novakovic et al., 2010, Silvestri et al., 2013). Physical and chemical characterization of these factors should be performed in short- and long-term experiments, while cross-referenced to other materials. Similar to cell-based therapy, the timing and the delivery method for biomaterials is important to maximizing therapeutic effects. MI substantially changes cardiac tissue and the local environment within hours and over a period of weeks (Kuraitis et al., 2010). The introduction of a biomaterial too soon could interrupt initial cardio-protective inflammatory and fibrotic cues following MI. However, it is found that material efficacy after severe remodeling and fibrosis in the later stages post-MI, with or without stem cells, is substantially reduced. Generally, injection or implantation should occur within 1 week after MI (Blackburn et al., 2015, Rane and Christman, 2011). Surgical implantation of a patch or prosthetic is an invasive procedure, which is less desirable than minimally invasive methods. Thus, intramyocardial delivery by injectable materials is an alternative, either by epicardial injection or catheter-assisted injection

(Hasan et al., 2015, Johnson and Christman, 2013). In time, new standards and strategies will elucidate the optimal procedures necessary for, at least partial, cardiac regeneration using biomaterials.

In order to maintain clinical relevance and momentum, it is critical to thoroughly evaluate the design philosophy and application of biomaterials. To this end, the work in this thesis characterizes the development of injectable hydrogels, comprised of non-animal source collagen, following a simple, reproducible, and time-efficient procedure appropriate for future translational cardiac therapy.

1.5 Rationale and Project Objectives

Injectable hydrogel biomaterials have emerged as promising therapies for regeneration of post-MI scar tissue. Collagen, a structural and functional component of the ECM, is a prominent choice for injectable matrices that can positively regulate inflammation, fibrosis, and remodeling of the MI heart. In our lab, rat-tail collagen type I based matrices have been shown to reduce inflammation, fibrosis, and improve neovascularization and cardiac function in the ischemic heart of mice and pigs in early-stage post-MI. However, these materials cannot be directly translated to humans due to the risk of toxins, immunogenic response, and batch-to-batch variability of the collagen source. Therefore, I hypothesize that a comprehensive de-novo protocol for the preparation of recombinant human collagen type I and type III (rHC TI and rHC TIII, respectively) injectable hydrogels can be developed to generate materials with suitable physical and functional properties for use in cardiac therapy.

The objective for this project was to develop a novel, biofunctional material that can act as a foundation for future cardiac therapies. To this end, the rHC TI and TIII hydrogels, in comparison to a porcine type I collagen (Theracol) hydrogel, were assessed for the following:

- Characterization of the collagen solutions
- Characterization of the collagen hydrogels
- Biocompatibility of the collagen hydrogels

Two important components for clinical relevance are human cell viability (biocompatibility) and transference technique (sterility, readiness, and ease of use). The use of recombinant human collagen and a t-piece mixing system in a stepwise protocol for injectable matrices is expected to satisfy these criteria. The emphasis on the translational aspect of these biomaterials is essential for advancement to the clinic.

2 Chapter: Materials and Methods

In this section, materials without a listed source are acquired from Sigma-Aldrich (Oakville, Canada). The majority of preparations for collagen solutions and hydrogels are completed in sterile conditions. This refers to the use of a biocabinet (AirCleanSystems®, H.E.P.A filtered), with standard sterilization using 70% ethanol. The three types of collagen prepared were porcine type I collagen (Theracol; Regenerative Medical System), recombinant human collagen type I (rHC TI; Fibrogen), and recombinant human collagen type III (rHC TIII; Fibrogen). These materials are manufactured following standard operating procedures (SOPs) that will continue to be revised throughout development.

2.1 Collagen Solution Consistency and Stability for Hydrogel Use

2.1.1 Preparation of collagen solutions

The collagen samples were freeze-dried prior to batch preparation. The rHC TIII was purchased from the manufacturer, Fibrogen, and the rHC TI was a gift from professor May Griffith (Montreal University). For Theracol, 35mL was transferred to 50mL centrifuge tubes (Corning). In preparation for lyophilization, the samples undergo pre-freezing in -80^{o}C temperature. The samples were inserted into individual vacuum chambers in a freeze dry system (LabConco). The samples were concentrated using this freeze-dried process requiring five days.

A 1.0% collagen solution is prepared by dissolving 0.1g of lyophilized collagen in 10mL of ultra pure ddH_2O (Sigma-Aldrich; DNase and RNase free, 0.1μm filtered). The

solution is left on a shaker overnight at 4°C. The samples completely dissolve in solution within 7 days. This constitutes one batch of collagen solution.

A 10mL BD syringe (Fisher Scientific) is used to prepare collagen solutions for making hydrogels. For sterilization, methanol (Fisher Scientific) is collected into the syringe five times, and then it is placed aside to dry. The plunger is submerged in methanol for 10 minutes, repeated twice. The plunger surface is wiped in between washing steps. The syringe components, separated, are left under UV for 30 minutes. Braun sealant caps (BBraun) are submerged in methanol overnight and attached to the syringe spout.

Plastic tubing (Thermo Scientific - Nalgene PVC) is placed on a glass dish. A razor is used to cut the tubing in 1.5cm segments, which are placed in 70% ethanol overnight with parafilm coverage. The tubing segments are collected using tweezers, and are dried on the glass dish. Prior to the first injection of collagen, the sealant cap of the syringe system is removed and one tubing segment is attached to the spout with tweezers. The tubing spout and the plunger entry are covered with parafilm before storage.

To ready the collagen for hydrogel preparation, the collagen solution is transferred to a 10mL pre-sterilized syringe with a sealant cap. The sealant cap and top opening are covered with parafilm. The solution is centrifuged in a Sorvall Legend RT (Fisher Scientific) at 484G for 15 minutes, repeated five times, and stored at 4°C. The plunger is inserted with assistance by a hypodermic needle the next day, before attaching the tubing spout. The completed collagen syringe (see Figure 2-1 for a schematic of the complete syringe system) is stored at 4°C at all times until used for hydrogel preparation.

2.1.2 Quality measure for pH of collagen solutions

The pH of each collagen stock (Theracol, rHC TI, and rHC TIII) was measured by pipetting a 10μL volume, which is smeared onto pH paper (MColorpHast^{TM} 0-14 indicator strip). This measurement is repeated for each batch of stock solution.

2.1.3 Measurement of absorbance for collagen solutions

Absorption spectra for Theracol, rHC TI, and rHC TIII stock solutions were measured in a Biochrom Libra S50 spectrophotometer. The blank and diluent for all measurements was Millipore Milli-Q deionized water at 18MΩ. For each test, a collagen solution at a 1:100 dilution was transferred to a quartz cuvette (Fisher Scientific; 18/B, 10mm path length), with a reading range of 200-400nm wavelengths. The peak wavelength (200nm) and lysine residue wavelength (220-222nm) were recorded.

2.1.4 Protein concentration for collagen solutions

The total protein concentration of the collagen stock solutions was measured using a Pierce^{TM} BCA Protein Assay Kit (Fisher Scientific). Standards and working reagent were prepared according to the manufacturer's protocol, following the microplate procedure. The standards were prepared from the albumin standard (2mg/mL bovine serum albumin in 0.9% saline and 0.05% sodium azide), within a working range of 20-2,000μg/mL. Collagen was prepared as 1:10 dilutions, in triplicate. Millipore Milli-Q deionized water at 18MΩ was the diluent for all standards and samples. For this protocol, 200μL of working reagent was mixed with 25μL of collagen sample per well. The microplate was covered in aluminum foil and incubated at 37^{o}C for 30 minutes. The

absorbance was measured at 562nm, using a microplate reader (Synergy Mx; BioTek). The protein concentration was determined from the standard curve generated by Gen5 Software.

2.1.5 Overall charge of collagen solutions

Collagen samples were diluted 1:100 in ultra pure ddH_2O and the zeta potential (mV) was measured with a dynamic light scattering Malvern Zetasizer Nano-ZS instrument.

2.1.6 Secondary structure of collagen solutions

Circular dichroism (CD) measurements of collagen samples diluted 1:100 in ultra pure ddH_2O were measured with a Jasco J-810 spectropolarimeter. Changes on the secondary structure of the collagen types were analyzed upon calculation of R_{pn} values (the ratio between 220 and 195.5 nm CD signals).

2.2 Collagen Hydrogel Production and Physical Analysis

2.2.1 Preparation of collagen hydrogels

The 1.0% (w/v) hydrogels are prepared using a t-piece system, represented by Figure 2-1. One t-joint (SciPro) has 3 inlets, which are locked with three cylindrical fittings (SciPro). A rubber septum (diameter: 0.5mm; ChromSpec) is placed in one of the horizontal fittings to seal the inlet. A 2.0mL glass syringe (Fisher Scientific) is attached to one of the open fittings, loaded with 1.5mL of 1X PBS. The PBS solution is injected into the system, with the excess expelled from the other opened inlet until a dome of PBS

remains. The PBS dome allows syringe attachment without introduction of bubbles. A hypodermic needle (18Gx6", Dyna Medical) is used to pierce the dome and eliminate air bubbles. Another glass syringe is prepared as above, which is attached to this opened fitting. The PBS is mixed between both syringes to remove air bubbles. One syringe is removed, containing the PBS, and the excess is expelled. This is repeated three times, alternating syringes.

When the system is equilibrated, the cold collagen stock (Theracol, rHC TI, or TIII) in a 10mL BD syringe is retrieved from 4ºC fridge. The third glass syringe is attached to the tubing end of the BD collagen syringe, and 1.0mL of collagen is transferred to the glass syringe. The glass syringe with collagen is connected to the t-piece system and mixed 20 times, repeated twice. An ice container cools the t-piece system throughout the procedure between mixing and injection stages. In a 1.0mL BD syringe (Fisher Scientific) with a sterile needle (BD Precision Glide; 25G x 1 1/2), 150µL of 1X PBS is added to the system via the rubber septum. The system is mixed 20 times, repeated twice. In a 1.0 mL BD syringe with a sterile needle (BD Precision Glide; 20G x 1 1/2), 100µL of 40% (w/v) Chondroitin Sulfate-C (CS-C; Wako) is added to the system via the rubber septum. The system is mixed 30 times, repeated twice. For the cross-linker, 500µL of 0.1M 2-morpholinoethane sulfonic acid monohydrate (MES) buffer (pH ~5.0) is added to the pre-weighed N-(3-dimethylaminopropyl)-N'-ethylcarbodiimide (EDC) and N-hydroxysuccinimide (NHS). The solution is mixed briefly using a vortex. Afterward, 200µL of NHS and EDC are mixed in a 1:1 ratio (11.7mM). In a 1.0mL BD syringe with a sterile needle (25G x 1 1/2), 200µL of EDC/NHS mixture is added to the t-piece system via the rubber septum. The system is mixed 20 times. The pH is adjusted (pH ~7.4) using

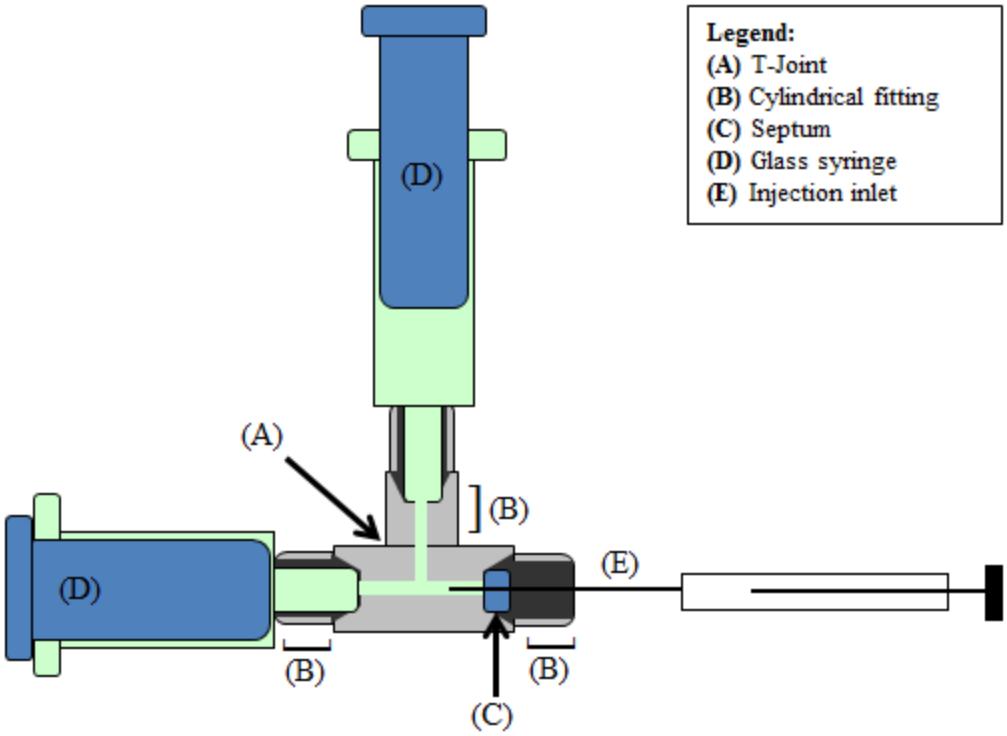

Figure 2-1: Schematic of t-piece system that contains and mixes hydrogel solution. A) The core of the mixing system, the t-joint, allows solution passage throughout mixing; B) the cylindrical fittings tighten the airspace at each t-joint opening and ensure firm closure with intact syringes; C) rubber septum seals one section of the t-joint and maintains closed environment; D) glass syringes contain hydrogel solution; E) injectable inlet is a space for introducing reagents to the hydrogel mixture. *modified image, originated from K. Merrett and M. Griffith.

0.1M NaOH. A total of 40µL (Theracol), 40µL (rHC TI), or 45µL (rHC TIII) is injected into the system. This is completed by maximum aliquots of 25µL per injection, using a 100µL Hamilton syringe via the rubber septum. The system is mixed 10 times with each NaOH addition, and then the reaction mixture is pumped into one of the glass syringes and removed from the t-joint. The mixture is transferred to a 6-well or 12-well plate (Corning) to solidify in an incubator at 37^{o}C or stored on ice for up to 45 minutes. The t-piece system components were cleaned using warm water and 0.1M HCl. The solutions were filtered (0.2µm) in sterile conditions with autoclaved Milli-Q deionized water.

2.2.2 Rheological characterization

The viscosity of the collagen hydrogels was measured using a Brookfield R/S Plus Rheometer. Hydrogels were prepared, stored on ice, and 200μL was transferred to the surface pedestal of the rheometer. The gel was then compressed with a C25-2/30 (conical) spindle, pre-calibrated at 4.0μm, with a constant 37^{o}C temperature control. A custom protocol measured rHC TI and rHC TIII, which consisted of a constant ramp shear rate (CSR) - (linear) with 1 unit / second from 5 to 300 units (1200 seconds). The viscosity of the gel was recorded in Pa•s. The hydrogels were measured until after gelation occurred, and an average maximum viscosity was recorded based on plateau readings uninterrupted by background signals.

2.2.3 Measure of cross-linker degree for hydrogels

The cross-linking degree of hydrogels, based on denaturation temperature (T_D), was measured using a Q2000 Differential Scanning Calorimeter (DSC; TA Instruments, New Castle, DE). Hydrogels were prepared and solidified in 12-well plates in an incubator at 37^{o}C, with an approximate thickness of 1.0cm, and then after gelation were covered with 1.0mL of PBS overnight at 4^{o}C. The PBS was removed from the surface and material was excised using a dimension cutter (0.5mm). The material was surface-dried using filter paper (Fisher Scientific) and weighed on a standard scale (5-20mg). The material was placed in an aluminum DSC sample pan (Tzero; TA Instruments) and hermetically sealed using an aluminum lid (Tzero; TA Instruments). The degradation cycle for each hydrogel was performed as follows: 1) baseline temperature of 25^{o}C, 2) temperature decline to 5^{o}C in 5 minutes, and 3) temperature ramp of increase of

5°C/minute for 15 minutes. Hydrogels were tested in triplicates with the T_D determined by the identification of an endothermic peak.

2.2.4 Hydrogel water content

The water content for the materials was determined by weighing the material before and after a drying process using a vacuum (Gast). The total water content (W_t) was calculated from the wet weight (W_0) and the dry mass (W), according to the equation:

$$W_t = \left(\frac{(W_0 - W)}{W_0}\right) \times 100$$

Hydrogel samples were excised using dimension cutter (0.5mm), and excess water was removed with filter paper. The samples were placed inside the vacuum container and dried over 24 hours at room temperature.

2.2.5 Enzymatic degradation of hydrogels

Enzymatic degradation of the collagen hydrogels was measured by collagenase digestion over time. Type I collagenase solution (5U/mL; Gibco) was prepared in Tris-HCl buffer (0.1M Tris-HCl and 5mM $CaCl_2$ at pH 7.4) and stored at 37°C. Prepared hydrogels in a 12-well plate were excised using a dimension cutter (20-40 mg) and placed into vials. The hydrogels were equilibrated for 1 hour in 5mL of Tris-HCl buffer at 37°C. The vials were filled with 1.0mL of collagenase solution and incubated at 37°C. The initial mass of each hydrogel was weighed at time zero, followed by weighing every 10 minutes over a 2-hour period. Collagenase solution was replaced after each sample was

weighed throughout the time period. The degradation rate (mg/min) was determined from the initial slope of the degradation slope.

2.2.6 Hydrogel Morphology

The architectural differences in the materials were observed by low temperature scanning electron microscopy (Cryo-SEM) in a Vega II - XMU (Tescan) instrument with a cold stage sample holder (-50^{o}C). In preparation, hydrogels were excised using a dimension cutter (0.5mm) and dried using filter paper before freezing at -80^{o}C. The sectioned samples, ~5mm thickness, were isolated in the SEM sample holder previously chilled with ice close to 0^{o}C. Images of the sectioned hydrogel samples were captured using a backscattered electron detector and a secondary electron detector. Pore size diameter, based on pore height and width, was measured from 300 individual pores using ImageJ® software.

2.2.7 Detection of NHS by-product release in hydrogels

The presence of chemical cross-linker after hydrogels solidification was measured in a Biochrom Libra S50 spectrophotometer. The blank, dilutions, and washes were carried out in 1X PBS. Hydrogels were prepared in 12-well plates, with 1.0mL of 1X PBS on the surface. A total of four washes were recovered, each for 45 minutes at 37^{o}C. For each test, supernatant at a 1:10 dilution was transferred to a quartz cuvette with a reading range of 200-400nm wavelengths. The presence of non-cross-linked NHS (260nm) was recorded.

2.3 Evaluation of the Collagen Hydrogels with Cardiac Relevant Cells

All procedures were performed with the approval of the University of Ottawa Animal Care Committee, in compliance with the National Institute of Health's Guide for the Care and Use of Laboratory Animals.

2.3.1 Cardiac fibroblast isolation and culture procedure

Cardiac fibroblasts retrieved from the hearts of 8-9 week-old female C57BL/6J mice (Jackson Laboratories) were used throughout the *in-vitro* investigation of the collagen hydrogels. The mice are sacrificed according to ACVS guidelines and hearts perfused with cold PBS, harvested in sterile conditions, and used for the following isolation process.

Cardiac fibroblasts were isolated from mice hearts immediately after animal sacrifice. Hearts were transferred to eppendorf tubes (Fisher Scientific) and minced using surgical scissors in 500µL of Hank's Balanced Salt Solution (HBSS without Ca^{2+} and Mg^{2+}; Thermo Scientific). Afterward, an additional 500µL of HBSS was added to the tube. The mixture of heart tissue was homogenized with a pipette, and then transferred to a 15mL centrifuge tube. The digestion solution is prepared with 2.5mL of HBSS and 1.5mL of digestion buffer (2.4U/mL Dispase II, 1mg/mL Collagenase B, 5M NaCl, 1M HEPES pH 7.5, ddH_2O). This 4mL digestion solution is added to the heart tissue mixture and incubated at 37^{o}C for 30 minutes. The contents are swirled every 5 minutes to ensure the minced pieces do not clump together. The mixture is homogenized with a pipette and passed through a 70µm cell strainer (VWR) into a 50mL centrifuge tube. An additional 30mL of HBSS is added to tube, which is centrifuged at 530G for 5 minutes. The

supernatant is aspirated and the pellet is transferred to a 100mm culture dish (Corning) with 10mL of Dulbecco's Modified Eagle Media/F12 (DMEM; 10% FBS, 1% penicillin and streptomycin, and 0.1% gentamicin). The culture dish is placed in an incubator at 37^{o}C for 5 hours before the media is aspirated and replaced.

Cardiac fibroblasts are maintained in an incubator at 37^{o}C until growth is maximized in the culture plate (*i.e.* until ~80% confluence). The cell cultures are then washed twice with 10mL of PBS (without Ca^{2+}/Mg^{2+}). These passage 1 (P1) cells are detached using 5mL of 0.025% trypsin (Gibco). The culture dish is placed in the incubator for 5 minutes. Once the cells are detached, 10mL of supplemented DMEM/F12 media is added to the culture dish. The culture solution is transferred to a 50mL Falcon tube and centrifuged at 300G for 5 minutes in a Sorvall ST16 centrifuge. The solution is aspirated and the pellet is resuspended with 1mL of supplemented DMEM/F12. The cells are added to a T-75 culture flask (P2; Corning) with 10mL of supplemented DMEM/F12, which is placed in an incubator at 37^{o}C until maximal growth is achieved. The cell media is changed every other day throughout this period.

2.3.2 Proliferation and morphology of cardiac fibroblasts on hydrogels

Collagen hydrogels (Theracol, rHC TI, and rHC TIII) were prepared and transferred to three 24-well plates that were incubated at 37^{o}C for 15 minutes. The preparation was made in triplicates, and 500μL of the aqueous hydrogel was transferred to one well. The experiment proceeded over a 5-day period, with each 24-well plate representing day 1, day 3, and day 5. The hydrogels were washed 4 times with 1mL of PBS over a 3-hour period. The hydrogels were stored at 4^{o}C overnight. Cardiac

fibroblasts (P2; in supplemented DMEM/F12) in a T-75 culture flask were washed twice with 10mL of PBS. The cells were detached with 5mL of 0.025% trypsin over 5 minutes in an incubator. Afterward, 10mL of supplemented DMEM/F12 was added to the flask and the contents were transferred to a 50mL Falcon tube. The cell suspension was centrifuged at 300G for 5 minutes. The supernatant was aspirated and the pellet resuspended in 1mL of supplemented DMEM F12. The number of cells was counted using a standard haemocytometer (Reichert), with 10μL of fibroblast suspension mixed with 10μL of Trypan Blue dye (0.4%; Beckman Coulter). The diluted cell suspension, ~5000 cells/mL as day 0, were seeded onto the hydrogels or tissue culture polystyrene (TCPS; control) in the 24-well plates with an additional 1mL of supplemented DMEM/F12. The media was replaced for the day 3 and day 5 plates on the second day and again for the day 5 plate on the fourth day. Images for the wells of each plate, on the respective days, were captured using a microscope (Zeiss Observer A1 Axio) on bright-field setting (20x magnification). For each well, 4 images of fibroblast morphology were obtained and cells were counted using ImageJ® software.

2.3.3 Cell stain imaging of cardiac fibroblasts on hydrogels

In order to improve the qualitative assessment, cell staining methods were applied to the proliferation experiment over a 5-day period. Following the procedure described in 2.3.2 above, hydrogels (Theracol, rHC TI, and rHC TII) were prepared and seeded with cardiac fibroblasts over a 5-day period. For the staining procedure, the plates were enclosed and covered with aluminum foil. The cells were washed twice with 1.0mL of pre-warmed PBS (37^{o}C at pH 7.4). The cells were fixed with pre-warmed

paraformaldehyde (4% PFA; 37ºC) for 10 minutes at room temperature under aluminum foil. The cells were washed with 1.0mL of pre-warmed PBS (37ºC at pH 7.4), repeated three times. Triton X-100 (0.1%) was diluted in PBS and transferred to the cells for 3 minutes. The cells were washed for a third time with 1.0mL of pre-warmed PBS (37ºC at pH 7.4) repeated three times. Wheat germ agglutinin cellular membrane stain (0.2% WGA-488; Fisher Scientific) and rhodamine phalloidin cytoskeleton stain (0.1%; Fisher Scientific) were prepared in PBS. The staining solution was added to the cells and incubated for 20 minutes at room temperature. The cells were washed with PBS, repeated twice. Nuclei stain 4',6-diamidino-2-phenylindole (1% DAPI) was prepared in PBS. After the cells were incubated with DAPI for 20 minutes, the solution was removed and the cells washed once with PBS. Images were captured using a fluorescence microscope (Zeiss Observer A1 Axio) with the following wavelengths: 365nm, 470nm, and 555nm.

Statistical Analysis

Comparisons of data between groups were performed with 1-way analysis of variance, and individual 2-groups comparisons were performed by a 2-tailed Student's t-test. Statistical significance was considered at $P < 0.05$. Values are expressed as means ± standard deviation.

3 Chapter: Results

3.1 Characterization of Collagen Solutions

The collagen preparation follows a quality control protocol that ensures that each batch of collagen is satisfactory for hydrogel production. Therefore, the physical properties of the stock solutions were tested prior to cross-linking. The properties evaluated for the collagen batches are listed in Table 3-1. The sterile, freeze-dried collagens were dissolved in ultrapure water to prepare 1.0% solutions. The solutions were colourless and viscous. Throughout storage (4^{o}C) over 6 months, the solutions remain visibly the same without any signs of bacterial contamination. The UV absorption spectrum has a maximum observed at 220nm for the collagen solutions. The BCA assays revealed a high protein concentration for Theracol, 3741.5 ± 80μg/mL, compared to the rHC solutions. However, similar protein concentrations between type I rHC, 626.2 ± 282μg/mL, and type III rHC, 703.1 ± 100μg/mL, were measured. The pH for the collagen solutions was within the acidic range (pH ~2-5) as acid soluble collagens. The CD spectra (200-240nm range) had a negative to positive pattern common in fibrillar collagens (Hwang et al., 2010, Fichard et al., 1997). The zeta potential measurements display a net positive charge for all collagen solutions. In summary, these tests were used to standardize and establish the quality of the stock solutions for preparing collagen intended for hydrogel production.

Table 3-1: Physical properties of Theracol, rHC TI, and rHC TIII stock solutions prepared for hydrogel production, showing qualitative characteristics, amino acid absorbance (220nm), total protein concentration (μg/mL), baseline pH, and zeta potential (mV).

Assessment	**Theracol Porcine Collagen Type I**	**Recombinant Human Collagen Type I**	**Recombinant Human Collagen Type III**
Qualitative	Colourless Viscous	Colourless Viscous	Colourless Viscous
Absorbance (220nm)	2.273±0.068 (n = 3)	2.120±0.120 (n = 3)	2.251±0.032 (n = 3)
Protein Concentration (μg/mL)	3741.5±80 (n = 3)	626.2±282 (n = 3)	703.1±100 (n = 3)
pH	2 (n = 3)	4 (n = 3)	4 (n = 3)
Zeta Potential (mV)	+23.9±1.90 (n = 3)	+3.7±2.60 (n = 3)	+12.4±2.60 (n = 3)

* Quantitative results are validated at an $n \geq 3$, and the mean is followed by the standard deviation

3.2 Optimization of the Collagen Hydrogel Protocol

The collagen hydrogels were prepared following a protocol that is designed, step-by-step, to ensure consistency and ease of use. The original protocol (Table 3-2) worked well for collagen from batch 1, but experienced problems with new collagen batches. To achieve a good standard, the hydrogels were prepared with numerous changes to pH, reagent concentrations, injection volumes, mixing repeats, and temperature (Table 3-3). The modifications were made one at a time, and successful changes were incorporated into the protocol. From this revision, there are some primary changes that resolved

hydrogel gelation complications. Importantly, adjusting the volume of NaOH, depending on the collagen batch and source, resulted in faster gelation and prevented cloudiness of the solution. In addition, NaOH aliquot injections compared to one total volume injection further complemented this modification. Also, changes to mixing order, such as CS-C before cross-linker, improved preparation and handling of the t-piece system. In particular, mixing duration was increased for most injection stages, which ensured uniform mixing for each newly introduced reagent. These changes streamlined the production method, which minimized temperature fluctuation for the t-piece system (maintained at 4^{o}C) and accelerated the preparation from start to finish. The finalized protocol, effective across different collagen batches with the appropriate adjustment to pH, produces high-quality gels with minimal bubbles (Table 3-4). The initial collagen-PBS mixture is colourless, and when CS-C is injected and mixed, the mixture retains its colourless, transparent appearance throughout gelation. The procedure is completed within 35 minutes, and the mixture crosslinks at 37^{o}C. It is estimated that the gelation time occurs between 8-10 minutes. The formed hydrogels are firm and stable without discolouration or cloudiness. This protocol was extensively modified, and the finalized procedure is streamlined for production of high-quality hydrogels in future applications.

Table 3-2: Original production method for Theracol, rHC TI, and rHC TIII hydrogels using the t-piece mixing system. For each stage, reagents are injected into the system with the appropriate volumes followed by mixing phases (all performed at 4ºC).

Stage	Reagent	Mixing
0	Equilibration (1X PBS) 150µL - 1X PBS	~10 times, displace bubbles
1	1.0mL - 1.0% Collagen	10 times - twice
2	150µL - 1X PBS	10 times - twice
3	200µL - 1:1 EDC/NHS	20 times
4	100µL - 40% CS-C	20 times
5	20µL - 1M NaOH	20 times
6	Prepared	-

Table 3-4: Stepwise overview for the final optimized production protocol for Theracol, rHC TI, and rHC TIII hydrogels using the t-piece mixing system. For each stage, reagents are injected into the system with the appropriate volumes followed by mixing phases (all performed at 4ºC).

Stage	Reagent	Mixing
0	Equilibration (1X PBS) 150µL - 1X PBS	~10 times, displace bubbles
1	1.0mL - 1.0% Collagen	20 times - twice
2	150µL - 1X PBS	20 times - twice
3	100µL - 40% CS-C	30 times - twice
4	200µL - 1:1 EDC/NHS	20 times
5	40-70µL* - 1M NaOH	10 times per aliquot
6	Prepared	-

* Volumes depend on type of collagen and batch - currently, Theracol (40µL), rHC TI (40uL), and rHC TIII (45µL)

Table 3-3: Overview of the modifications to the hydrogel production protocol that were tested. Most of the trials were completed first using Theracol, and then followed up to confirm the same outcome with rHC TI and rHC TIII.

Collagen Batch	Modification	Outcome
1	No modification – see Table 3-3	Transparent, minimal bubbles and proper gelation
2	Original method w/ and w/o t-piece mixing system (pipette mixing)	Poor gelation – hydrogels appear cloudy, fail to solidify with more bubbles
	Original method w/ and w/o 40% CS-C (100µL 1X PBS substitute)	Poor gelation – slight pH increase, hydrogels remain cloudy
	New buffers and reagents (filtered, sterilized)	No contamination, hydrogels remain cloudy, fail to solidify
	EDC/NHS ratio (1:1) changed to 25mg/15mg, respectively	Gelation improved (semi-solid), but time ~45min, still cloudy
	Original method – w/ additional 100µL of 1X PBS (400µL total)	Increased pH (appeared at 7.2 vs. 7.0); otherwise no change
	Original method – w/ 30µL or 40µL of 1M NaOH w/ 300µL 1X PBS	Cloudiness dissipates, 30µL – gelation within 20min 40µL – gelation within 25min
	Original method – w/ 100µL 20% CS-C	Gelation time ~25min, but hydrogels are too soft
	Method order – 40% CS-C injected before EDC/NHS solution	Improved preparation time for cross-linker
	Mixing number – increased for collagen, PBS, CS-C, and EDC/NHS stages	Improved gelation time(18min), mixture homogeneity improved
3	Method 2.0 – method order, mixing number, 40µL NaOH, 300µL (total) PBS, 100µL 40% CS-C	Poor gelation – time ~40min (semi-solid) for bubbly, cloudy hydrogel
	New buffers and reagents (filtered, sterilized)	No contamination, no difference in hydrogel
	Method 2.0 – w/ 30µL 1M NaOH	No difference in hydrogel
	Method 2.0 – w/ pH investigation (range of detectors)	Mixed pH results (6.2-7.4) with hydrogel repeats
	Method 2.0 – 150µL 1X PBS mixed w/ phenol red pH indicator	NaOH range (40-120µL), verified 70µL optimal (~7.2), hydrogel still cloudy
	Method 2.0 – w/ the addition of aliquoted NaOH (1/3 of total per injection into system), w/ more mixing	Improved gelation (15min), cloudiness dissipates
	Final method – temperature: increased mixing speed and exposure to ice	Reduced occurrence of semi-solid gelation in trials

3.3 Characterization of Collagen Hydrogels

3.3.1 Physical and mechanical properties of collagen hydrogels

Rheological properties are important to understanding material physical features attributed to the composition of a hydrogel material. Rheology can provide information such as viscosity and time to gelation, which are important in determining the injectability of a material and the time one should work with the material before it solidifies. The chemical cross-linking of the rHC hydrogels alters these properties during aqueous to solid phase transition. Therefore, the viscosity (Pa•s) of the collagen hydrogels was examined, considering the intended use of the hydrogels for injection and spreading within the myocardium. The data analysis demonstrated that the rHC TI and TIII hydrogels have a significantly greater maximum viscosity compared to the type I porcine collagen (Theracol). Furthermore, the maximum viscosity was greater for rHC TIII compared to rHC TI. Using the same concentration of cross-linker, the viscosity increased from Theracol to rHC TI to rHC TIII (Fig. 3-1). The viscosity was determined using multiple points along the plateau (maximum) during the trials. The shear rate (1/s) applied (within 3-350 units) to generate the maximum viscosity readings differed for each type of hydrogel, indicative of material differences, although the parameters were the same. The difficulties affiliated with the gelation measurements are explained in the discussion.

The material composition (% source) and cross-linker (concentration, type) dictate the mechanical properties of a hydrogel upon gelation. However, water absorbent materials impart properties similar to natural tissues. Once polymerized, the collagen matrices are highly water absorbent and flexible materials. The water content of a

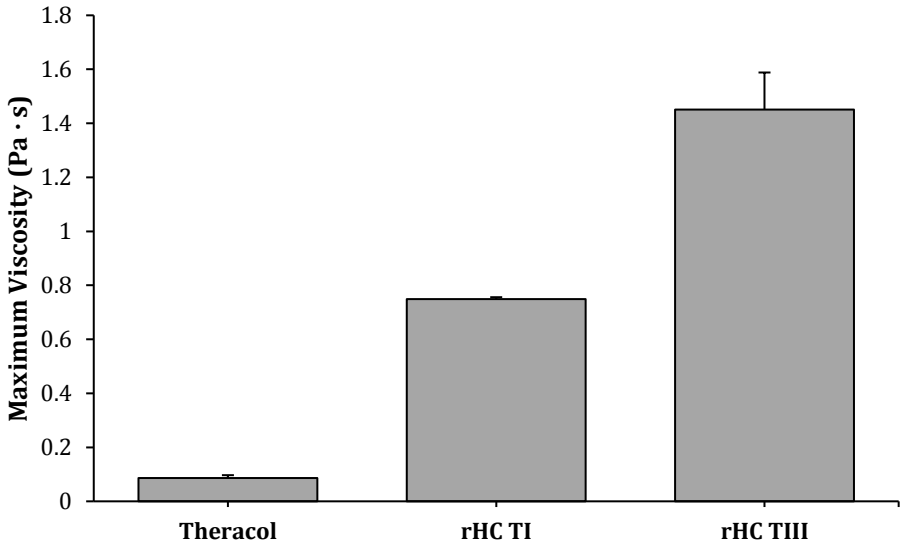

Figure 3-1: Maximum viscosity (Pa · s) of Theracol (n = 2), rHC TI (n = 1), and rHC TIII (n = 1) hydrogels measured 10 minutes after gelation at 37ºC. Parameter: shear rate (1/s), ramp setting of 5-350 units over 1200 seconds.

hydrogel, affected by material composition and cross-linking efficiency, can promote material-environment interactions in a living, dynamic system. To assess water content, hydrogel samples, under vacuum, were weighed before and after dehydration to ascertain wet and dry weight for total water content (%; see 2.2.4). The water content for Theracol was 94.72%, for rHC TI was 83.76%, and for rHC TIII was 93.96%. The hydrogels have a high water absorbance (> 90%), with no significant difference between them (Fig. 3-2). There was no relationship between type and source of collagen that influenced water content. The dry weight materials were quite brittle and stiff, while the wet weight materials were flexible and soft. Overall, the hydrogels are primarily comprised of water.

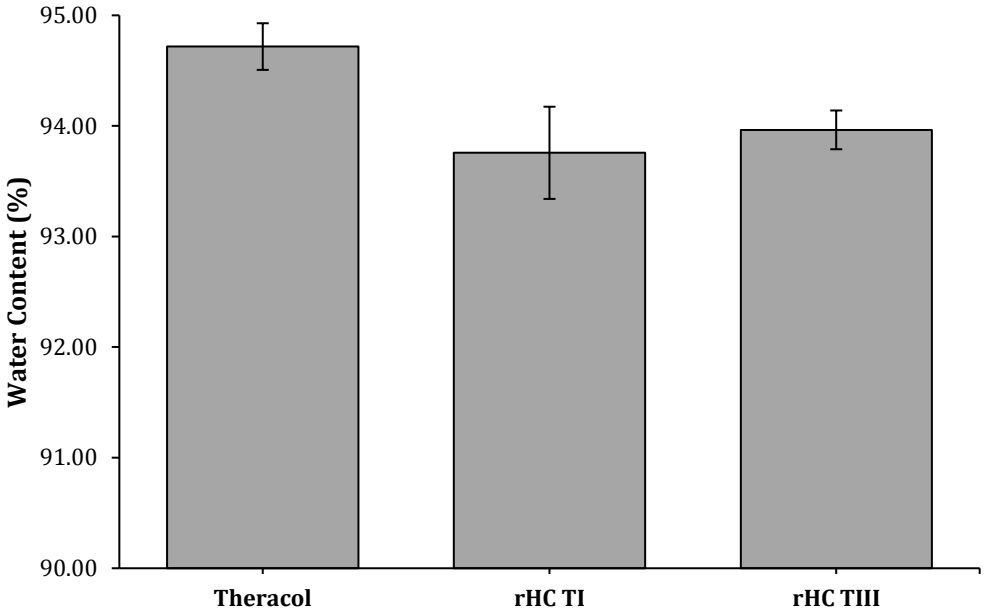

Figure 3-2: Water content (%) of Theracol, rHC TI, and rHC TIII hydrogels. Sample size is $n \geq 3$, with associated standard deviations.

3.3.2 Material degradation features and cross-linker efficiency

The collagen matrices form polymerized networks throughout gelation, which is facilitated by a thermal response (37^{o}C) in the presence of chemical cross-linkers EDC and NHS. The covalent amide bonds of the inter-connected collagen create a strong and flexible network that enhances material mechanical properties. However, the extent of cross-linking during the gelation period and material stability are factors that pertain to its *in-vitro* and *in-vivo* applications. Temperature-dependent degradation (T_D) of the collagen hydrogels can be used to determine cross-linking degree. The T_D of the hydrogels, the point at which denaturation begins, is detected by the presence of an endothermic peak. This is apparent by a negative heat flow (W/g) shift over a temperature increase by the calorimeter. The data analysis using three different batches of collagen demonstrates that the hydrogels remain stable above physiological temperatures

(Fig. 3-3). All materials had a T_D in the range of 40 to 60°C. There is no significant difference in cross-linking degree between batches of Theracol, rHC TI, and rHC TIII.

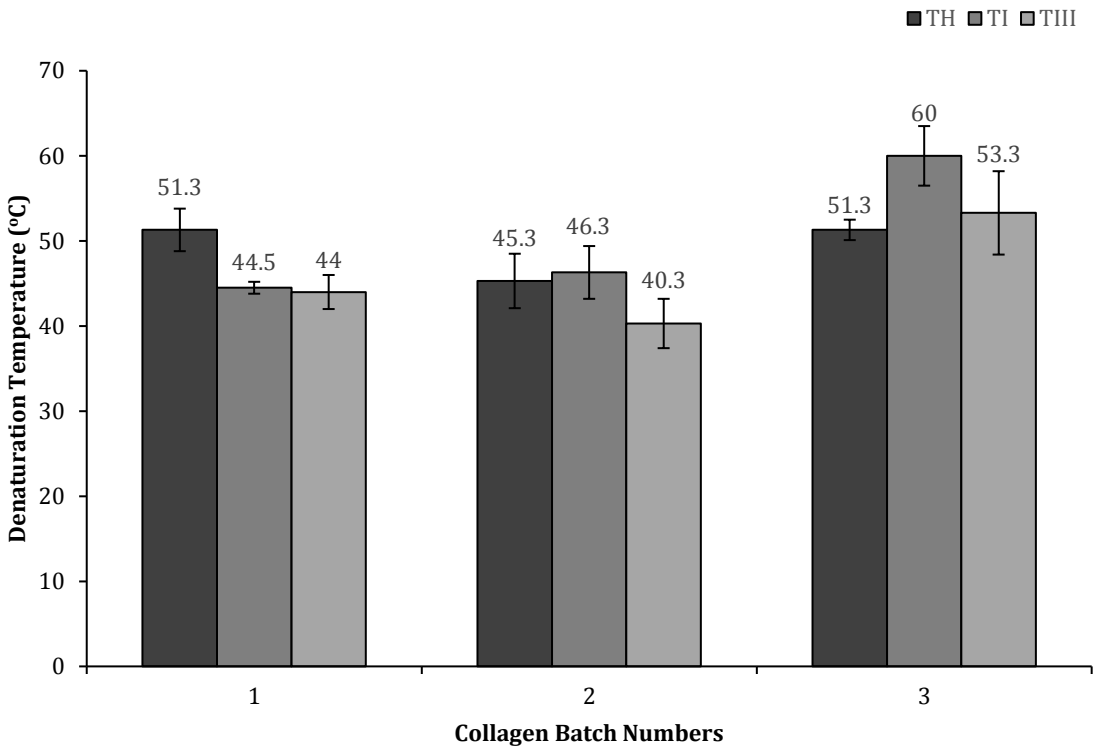

Figure 3-3: Denaturation temperature (T_D) of Theracol, rHC TI, and rHC TIII hydrogels from three different batches of collagen solutions. Parameter: 5°C/min ramp, maximum 80°C. Sample size is $n \geq 3$, with associated standard deviations. No statistical significance between groups for rHC hydrogels and Theracol was found.

Collagen, like other proteins, is susceptible to degradation by enzymes within a biological system. In particular, collagenases are enzymes that target the peptide bonds of collagen. The rate of degradation by collagenases on the hydrogels can represent the stability of the cross-linked material at physiological temperature. Therefore, the degradation of the different collagen hydrogels in response to collagenase treatment was tested. The effect of collagenase (5U/mL) was different for each hydrogel. In order, degradation by dry mass is fastest to slowest for rHC TI, Theracol, and then rHC TIII

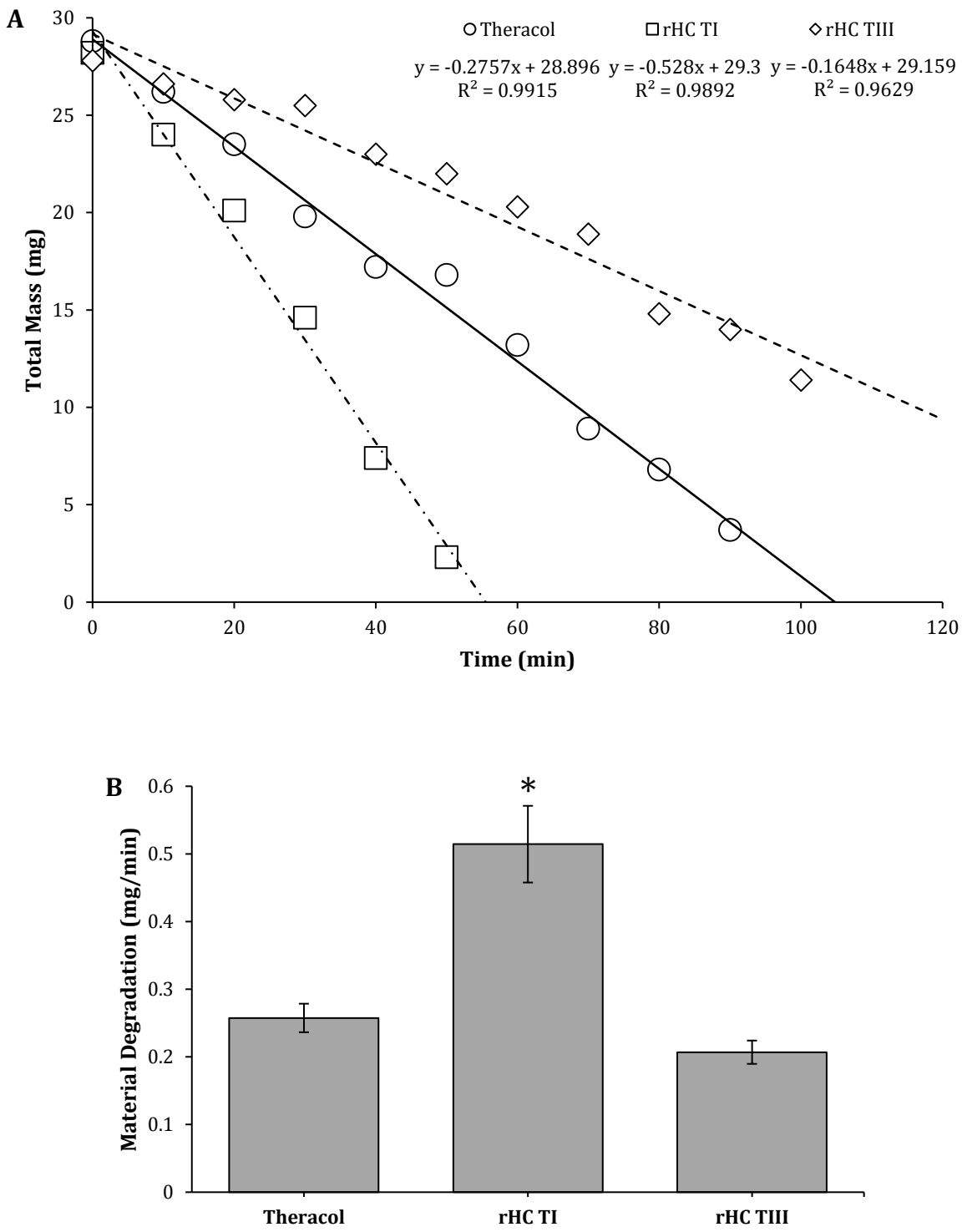

Figure 3-4: A) Enzymatic degradation of Theracol, rHC TI, and rHC TIII in collagenase solution (5U/mL) over 2-hour incubation period at physiological temperature (37°C). B) Material degradation (mg/min) of Theracol, rHC TI, and rHC TIII in collagenase solution (5U/mL). Sample size is $n \geq 3$, with associated standard deviations. * $P < 0.05$ *vs.* Theracol and rHC TIII.

(Fig. 3-4 A). The rate of degradation (Fig. 3-4 B) is significantly greater for rHC TI compared to rHC TIII (2.49 ± 0.5-fold; P = 0.0004) and Theracol (2.00 ± 0.7-fold; P = 0.002). There is no significant difference in degradation rates between rHC TIII and Theracol. The rate of degradation is unaffected by differences in initial hydrogel mass.

The use of chemical cross-linkers can lead to the release of unreacted by-products during hydrogel gelation. The presence of unreacted EDC or NHS indicates less than 100% cross-linking efficiency based on excess volume introduced or limited sites for reaction to commence. Therefore, the presence of chemical by-products was examined by UV-Vis using washes from prepared hydrogels (Fig. 3-5). The hydrogels exhibited similar absorbance profiles (200-400nm), with a broad peak at ~260nm (unreacted cross-linker) and a narrow peak at ~210nm (collagen). For each spectrum, the absorbance intensity decreases considerably after the 2nd wash. Furthermore, the presence of the broad peak diminishes significantly after the 4th wash. The spectra pattern for all washes is similar for Theracol, rHC TI, and rHC TIII.

3.3.3 Material micro-architecture

The rHC hydrogels are intended to establish a stable environment that facilitates cellular health and function. Therefore, the dynamic cell-material interactions are influenced by the micro-architecture of the hydrogel. The physical architecture of the cross-linked hydrogels is dependent on the cross-linking degree, which affects pore size and the permeation of substances. The cross-linking procedures for rHC TI and TIII are the same, yet the differences in the collagen polypeptide chain structures can result in varied micro-networks post-gelation.

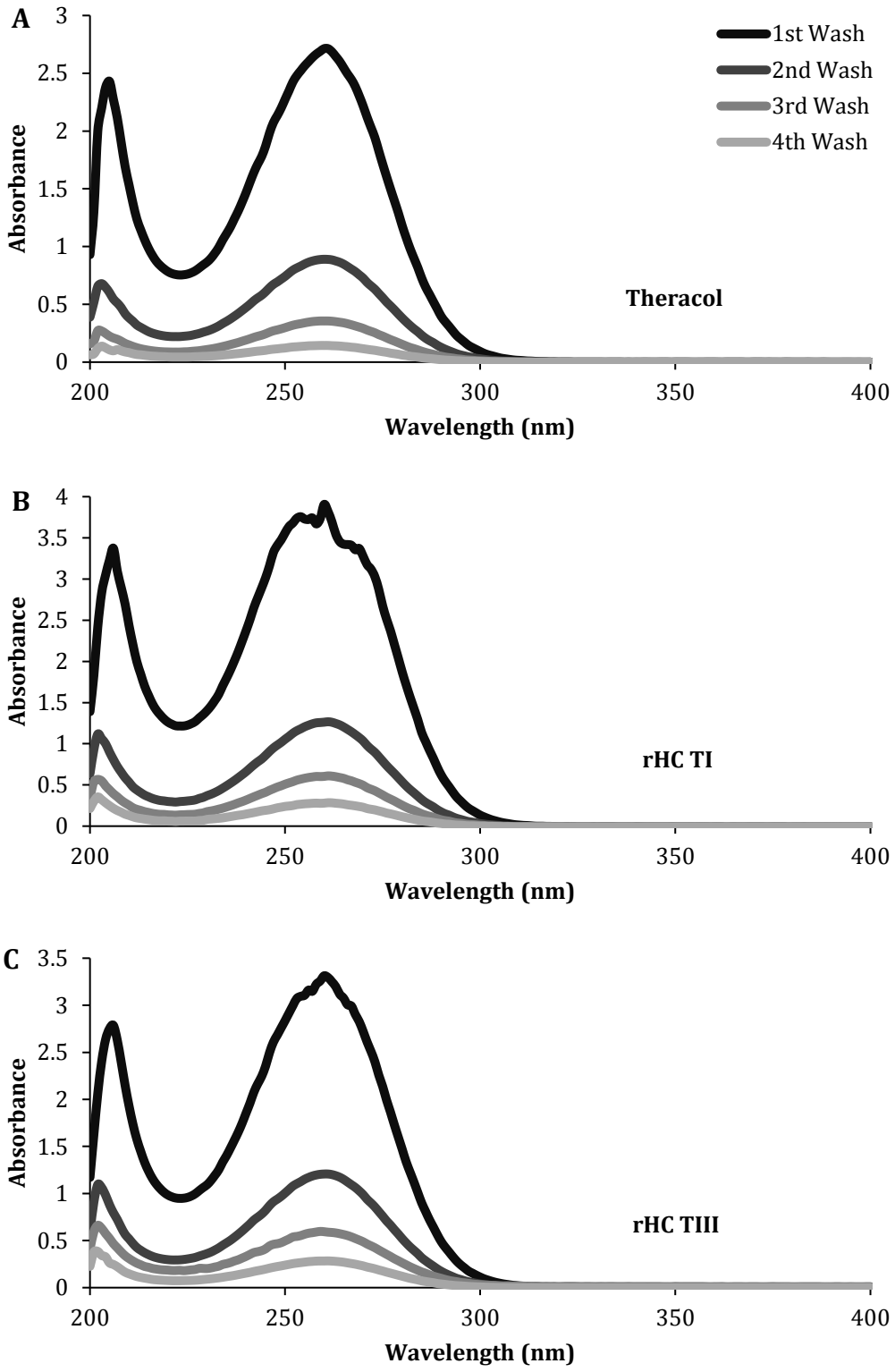

Figure 3-5: Detection of chemical cross-linker by-product release from A) Theracol, B) rHC TI, and C) rHC TIII hydrogels following 4 washes with 1X PBS at physiological temperature (37°C). Absorbance readings (260nm) were measured with 10X dilutions of the PBS washes.

Collagen hydrogel samples were frozen and fractured to visualize sectioned pore dimensions created post-gelation (Fig. 3-6). The representative images were captured at the micro-scale (500μm). The architectural differences were quantified by measurements of average pore size dimensions (height and width) for Theracol, rHC TI, and rHC TIII (Fig. 3-7). Theracol pore dimensions were larger (H: 12.6 ± 0.5μm / W: 12.4 ± 0.4μm; $P < 0.005$) compared to rHC TI (H: 9.5 ± 0.3μm / W: 10.5 ± 0.4μm). Furthermore, rHC TIII pore dimensions were significantly larger (H: 27.3 ± 1.0μm / W: 24.2 ± 0.9μm; $P < 0.0001$) compared to Theracol and rHC TI. These size differences are notable in the images. Theracol contained pores of different shapes and sizes throughout the network (Fig. 3-6 A). For rHC TI, the network appears as a sheet of small pores inter-connected in an organized pattern (Fig. 3-6 B). For rHC TIII, the pores appear as bulky, elongated spots clustered together (Fig. 3-6 C). Therefore, it appears that the source and structure of collagens influences the cross-linked physical architecture.

3.4 Biocompatibility of Collagen Hydrogels

3.4.1 Support and growth of mouse cardiac fibroblasts on rHC hydrogels

The rHC hydrogels are intended to act as a scaffold support to reduce inflammation and fibrosis, promote cell angiogenesis and tissue neovascularization, and to improve cell survival at the infarct site. Prior to testing the regenerative properties and injectable performance (*in-vivo*), the scaffolds need to display acceptable *in-vitro* biocompatibility with relevant cardiovascular cell lines. Therefore, hydrogels produced with the finalized, optimal protocol were subjected to an *in-vitro* assessment of their ability to support mouse cardiac fibroblasts.

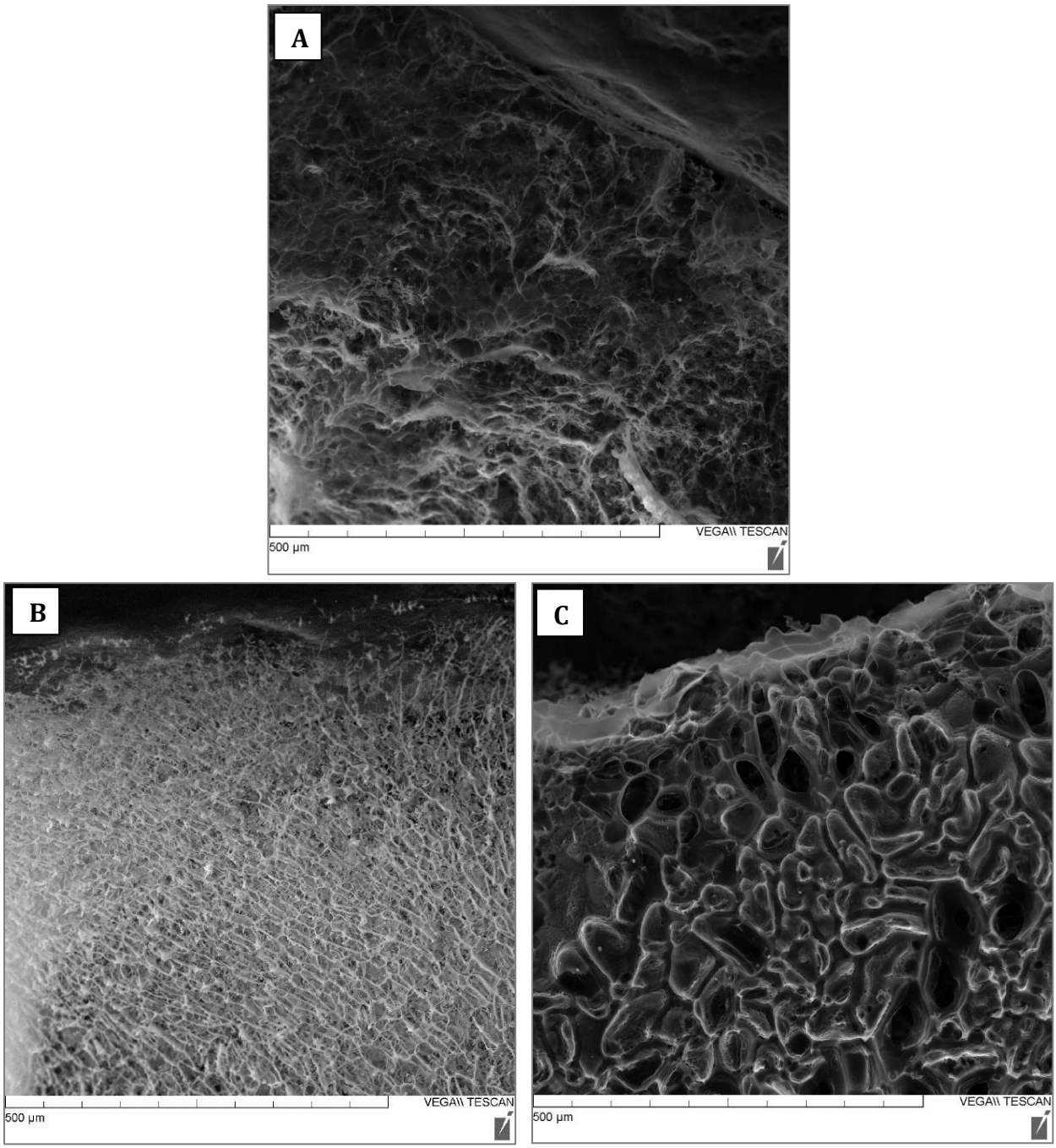

Figure 3-6: Cryo-SEM images of the micro-architecture for A) Theracol, B) rHC TI, and C) rHC TIII hydrogels. Representative images are captured at 300X magnification, scale bar 500µm.

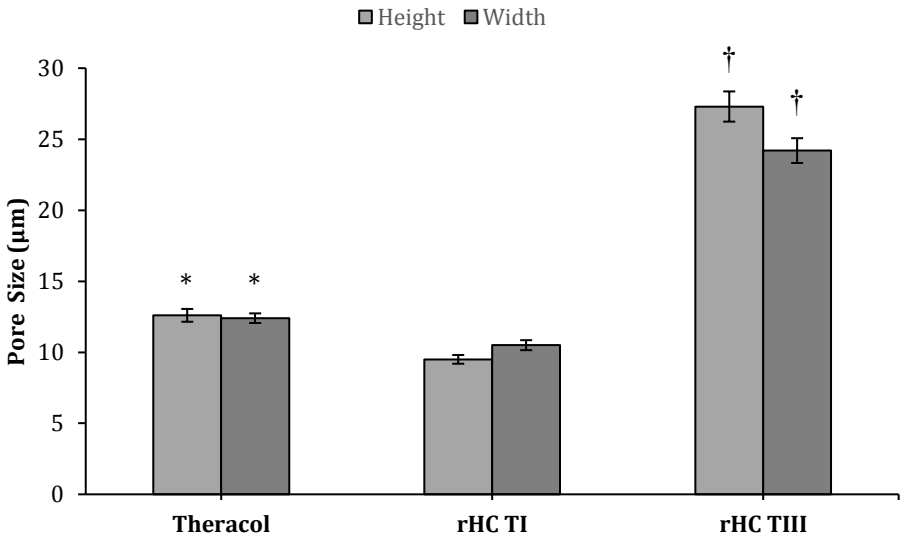

Figure 3-7: Pore size dimensions (height and width) for Theracol, rHC TI, and rHC TIII hydrogels. ImageJ® software was used for three images and > 200 pores measured per hydrogel. * $P < 0.005$ *vs.* rHC TI, † $P < 0.0001$ *vs.* Theracol and rHC TI.

Observation of the cultured cells (cell seeding density at day 0: ~5000 cells/well) on rHC TI and rHC TIII compared to a control culture (TCPS) were carried out over a 5-day period. The cell images were captured on day 1, day 3 (not shown), and day 5 for the culture period. Representative images show that cardiac fibroblasts on the rHC hydrogels are proliferative and healthy by the end of the period (Fig. 3-8). On day 1, the fibroblasts on the rHC hydrogels appear to grow dispersed on the surface compared to the typical aggregated growth on the control. On day 5, the cells grow together in patches on rHC hydrogels. Theracol (not shown) displayed limited cell growth on day 1, which improved by day 5 comparable to the rHC hydrogels. The cells on rHC TI and TIII adhere with a thin, stretched morphology in patches compared to the control, which are clumped together. This morphology is more apparent with fine adjustment of the lens focus. The cells growing on the rHC hydrogels were not only found on the surface, but within the

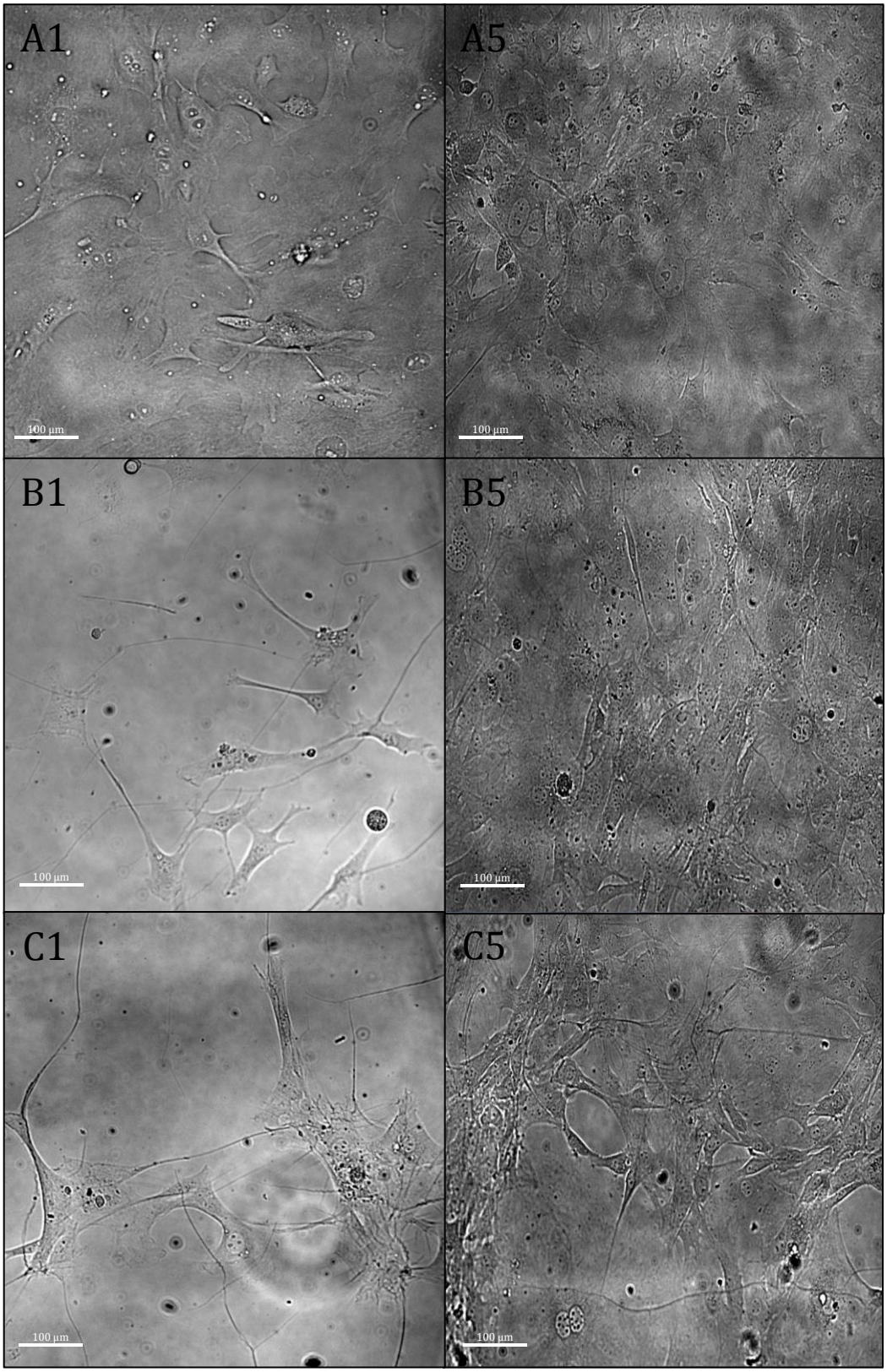

Figure 3-8: Cardiac fibroblast morphology comparison for A) Control, B) rHC TI, and C) rHC TIII after 1 and 5 days of culture. Representative images are captured at 20X magnification.

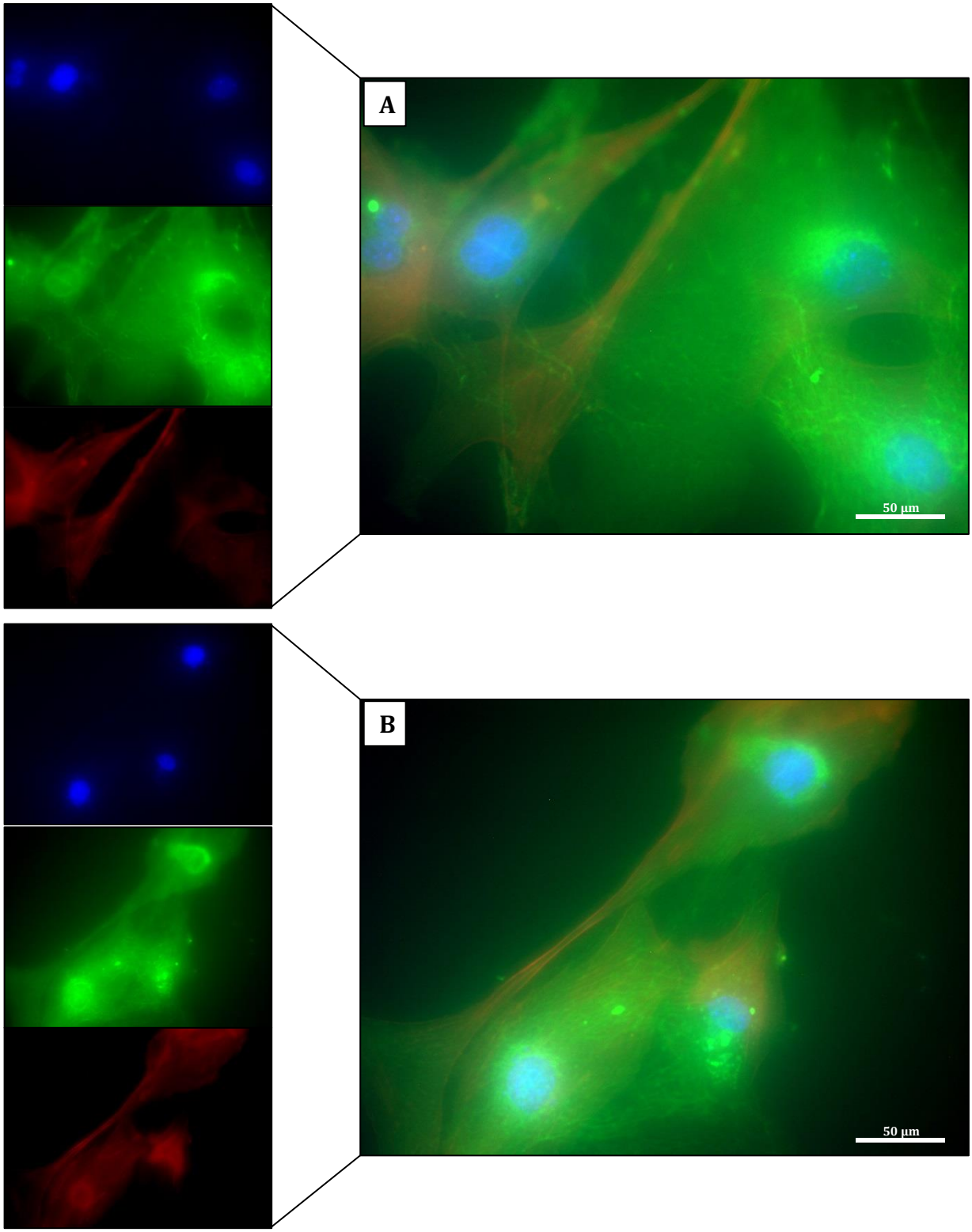

Figure 3-9: Representative images of cardiac fibroblasts seeded on A) rHC TI hydrogel and B) rHC TIII hydrogel on day 3 of culture. Left, single channel cell staining images of top: DAPI-stained nuclei (blue), middle: WGA-488-stained membrane (green), and bottom: rhodamine phalloidin-stained cytoskeleton (red). Right, merged image of all 3 channels. Representative image captured at 40X magnification.

hydrogel itself. Cell-staining immunohistochemistry techniques were applied to better visualize fibroblast growth and interactions with the rHC hydrogels. The nuclei (DAPI), cellular membrane (WGA-488), and cytoskeleton (rhodamine phalloidin) were co-stained in fixed cells. The representative composite images (Fig. 3-9) show healthy fibroblasts on the surface of rHC TI and rHC TIII hydrogels at day 3. The surrounding membrane envelops the cell with an inter-connected cytoskeleton extending throughout the fibroblast. The imaging for rHC TI and rHC TIII were comparable to the control, demonstrating that the rHC hydrogels support fibroblasts that exhibit typical spindle-shape morphology.

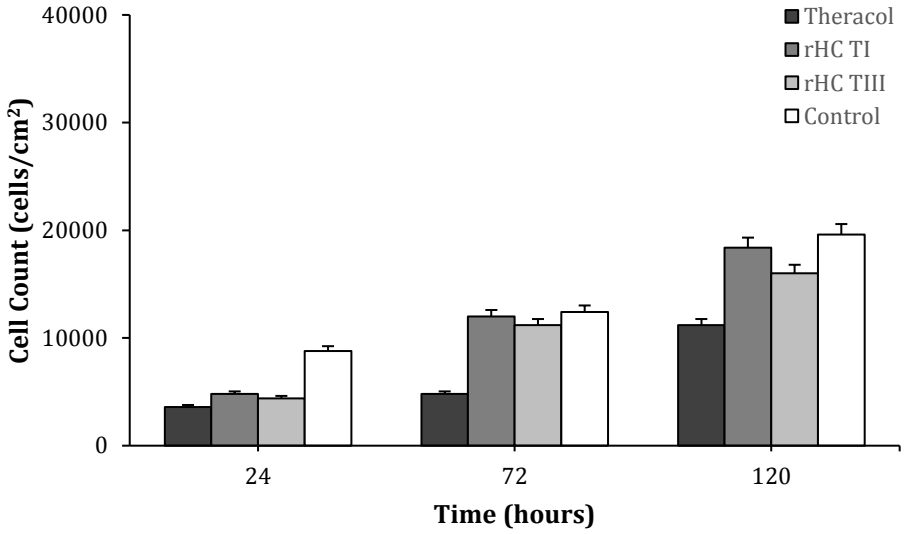

Figure 3-10: Cardiac fibroblast cell number measured over a 5-day period after cell seeding on empty plate (control) or on thin layer (1mm) of Theracol, rHC TI, and rHC TIII.

The proliferation data analysis further demonstrates fibroblast growth on the rHC hydrogels during the 5-day period (Fig. 3-10). Initially, at day 1 of culture, the cell growth was limited on the hydrogels compared to the control. This remained for Theracol throughout the trial. However, the cell growth on the rHC hydrogels remained similar to each other and to the control on day 3 and 5. Proliferation does not appear to be affected by interaction with the rHC hydrogels compared to the standard culture substrate (TCPS). Therefore, the rHC hydrogels display an ability to support cardiac fibroblasts.

4 Chapter: Discussion

4.1 Significance and Interpretations

Biofunctional scaffolds, specifically injectable hydrogels, hold great promise for the repair and regeneration of post-MI cardiac tissue. However, only a few proposed materials have partially accomplished this task to date within clinical relevance (Perea-Gil et al., 2015). The obstacles that hinder the development process must be addressed in order to meet future demands in cardiac therapy. In part, it is necessary to innovate material preparation with parallel focus on translational and experimental design throughout an investigation (Hasan et al., 2015, Johnson and Christman, 2013). In this study, injectable hydrogels comprised of recombinant human collagen type I and type III were compared to evaluate differences in physical and chemical characteristics alongside compatibility with cardiac fibroblasts. The materials were prepared using techniques that are transferable to a clinical setting. Overall, the study outcomes determined that: 1) non-animal source rHC, with minimal batch-to-batch variability, was viable for hydrogel production using a specialized t-piece system; 2) characterization of the 1% rHC TI and TIII hydrogels show similarities and differences in cross-linking degree, polymeric architecture and other physical properties; 3) rHC hydrogels demonstrate a capacity to support the growth, proliferation, and proper morphology of seeded cardiac fibroblasts. These findings act as a foundation for novel material design intended to establish a standard in clinical and experimental biomaterials for cardiac therapy.

One of the foremost aspects to this novel development is the collagen source for the investigated hydrogels. Animal-derived (porcine, bovine, rat, *etc*.) collagens are common sources for biomaterial design, and although sometimes acceptable in exterior

applications (*e.g.* skin formulations for scars, burns, and grafts) these sources pose a high-risk for immunogenic and inflammatory responses innate to foreign substance detection (Yang et al., 2004). Manufacturers have difficulty in ensuring large-scale production of animal-derived substances without risk of contamination (*e.g.* viruses, prions) and conservation (*e.g.* batch quality, variability) that affect product safety and performance (Liu et al., 2006, Yang et al., 2004). Furthermore, the sensitivity to animal-derived products varies between individuals and thus challenges standardization. This cannot undermine the potential of animal-derived hydrogels (Perea-Gil et al., 2015, Seif-Naraghi et al., 2013); nonetheless this risk is unacceptable for long-term inquiries in human cardiovascular scaffolds. The additional inflammation or damage to infarcted and ischemic tissues that animal-based products may confer is counter to TERM requirements. These considerations are pertinent due to the expected engraftment time and ensuing degradation of scaffolds. The prospect of biosynthetic rHC lies in its formation of human collagen matrices for human tissue 3D microenvironments (Yang et al., 2004). The techniques for rHC replication reliably create high purity, specific collagen types with matching amino acid sequences to human origins. Furthermore, modifications to the collagen sequences can provide application specific alterations for improved performance (Yang et al., 2004). The application of rHC in tissue engineering, such as dermal wounds (Nuutila et al., 2015) and cartilage repair (Muhonen et al., 2016), has been steadily increasing over the last decade (An et al., 2014, Yang et al., 2004). In particular, rHC has successfully been used in corneal replacement procedures that positively improve visual acuity without rejection or infection in long-term studies (Fagerholm et al., 2014, Fagerholm et al., 2010). For this study, collagen TI and TIII

were chosen because they are integral to healthy ECM structure and function in the native heart. Post-MI, the ratio of TI/TIII changes and consequently influences cardiac remodeling and fibrosis (Lopez Salazar et al., 2006, Pauschinger et al., 1999, Wei et al., 1999). The investigation of collagen TIII for use in cardiac biomaterials has been minimal, prompting an opportunity to evaluate its potential in comparison to the better-defined collagen TI materials.

The rHC TI and TIII batches were evaluated for quality and consistency. Overall, the rHC solutions were conserved and quite similar to each other. No indication of fibrillogenesis was present, since the rHC solutions have a low pH of 4, and also supported by the observed net positive zeta potential that was stable in water. Furthermore, the CD spectra displayed the expected pattern for triple-helical structures in collagen (Usha et al., 2012). Qualitatively, the homogenous rHC water solutions exhibit defined transparency and clarity while rHC TIII is more viscous compared to rHC TI. This factors into the structural differences between these rHC types and affects cross-linking degree and hydrogel characteristics. In summary, these tests revealed no defects in rHC TI and TIII compared to Theracol. This moved the development forward into hydrogel production.

In addition, another aspect important to this development was the production and post-production route. Transference methods for cardiac tissue engineering materials are a complicated and multi-faceted issue for clinical relevance. Post-MI patients have experienced a traumatic event, and likely have or will undergo preventative operations to minimize acute consequences. It is undesirable to include additional invasive procedures, which in itself may contribute to adverse remodeling or inflammatory complications.

From this perspective, injectable hydrogels are ideal (Hasan et al., 2015, Radhakrishnan et al., 2014). Qualities from the aforementioned section describe the benefits imparted by hydrogels. The aqueous composition prior to gelation allows for minimally invasive, localized delivery. However, preparations must adhere to time and mobility restraints for cardiac therapy. Biomaterials should be prepared in a sterile, enclosed environment to eliminate exterior contamination. Furthermore, the method should be minimalistic and compact for ease of use. In this study, these conditions are met with the use of the t-piece mixing system (Fig. 2-1). For 1% collagen solutions, the mixing pressure and turbidity are managed within the system. The t-joint and cylindrical fittings create an air-sealed space for homogenous mixing of the hydrogel solution between glass syringes. The septum allows for reagents to easily be introduced without compromising the mixture. The portable system can be used in any setting, and the resulting mixture transferred to a syringe prior to gelation. The thermo-responsive hydrogel remains aqueous on ice for short-term storage, providing flexibility for injection procedures. Although the hydrogel production protocol required revisions, the t-piece system did not contribute to these complications. In future pre-clinical studies, this system will be ideal in hydrogel production standards. For this project, these two aspects create the core of the development process. To date, no hydrogels comprised of either rHC TI or TIII have been reported for injectable cardiac therapies.

The rHC hydrogels are thermo-responsive and chemically cross-linked to form soft, 3D polymeric networks. Unique to hydrogels, gelation mechanisms are activated by physical, chemical, or biological cues that induce matrix polymerization. For this study, hydrogels were cross-linked using EDC/NHS chemistry. EDC is a carbodiimide and NHS

is an active ester, which both facilitate the formation of amide bonds in the presence of carboxylic (*e.g.* aspartic and glutamic acid residues) and amine (*e.g.* hydroxy(lysine) and lysine residues) functional groups exposed by collagen polypeptide chains. Importantly, the resultant unstable carboxylic ester (O-acylisourea intermediate) is displaced by amine-reactive NHS-esters that improve the cross-linking efficiency (Olde Damink et al., 1996). This type of covalent, chemical cross-linking is thoroughly assessed for collagen biomaterials (Delgado et al., 2015, Shepherd et al., 2015, Usha et al., 2012). Our lab group has presented *in-vitro* and *in-vivo* biomaterials cross-linked by EDC/NHS chemistry without mechanical or biological complication (Blackburn et al., 2015, McEwan et al., 2011, Deng et al., 2010, Suuronen et al., 2009). Importantly, this mild chemical reagent is not interwoven in collagen linkages and therefore does not persist after gelation nor alter the collagen structure (Davidenko et al., 2015, Usha et al., 2012). The cross-links formed are zero length inter- and intra-helical amide bonds that improve structural stability upon complete gelation (Shepherd et al., 2015, Usha et al., 2012). Therefore, this polymeric network strengthens the mechanical properties and degradation resistance.

The hydrogels were all produced following the same procedure, summarized in the final stepwise protocol (Table 3-4). However, modifications were necessary to reach this consistent, high-quality protocol. The matrix solution must be compatible with the cardiac physiological environment. Therefore, the hydrogel solutions are mixed with sterilized PBS, MES, CS-C, and NaOH. The glycosaminoglycan chondroitin sulfate is an important biological polymer that assists in the structural stability of functional biomaterials. The basic, ionic salt adjusts the pH of the hydrogel mixture (relatively

acidic after cross-linking reagents) to ensure physiological pH of ~7.4. This is performed using the t-piece mixing system, which ensures precise injected volumes. The consistency issue demonstrated during hydrogel production was apparent after using new collagen batches. The hydrogels failed to polymerize, and only formed soft, cloudy slurries after an extended period (not shown). It was at this stage in the project that I revised the hydrogel production technical details. Following systematic elimination, the corresponding physical and chemical components involved in the hydrogel mixture were modified. The changes that provided some resolution for gelation issues included pH adjustments, mixing number (duration), and reagent order. The mixing phases ensure that with each reagent addition the mixture is homogenous. Preferably, CS-C is injected prior to EDC/NHS to avoid premature cross-linking throughout the remainder of the protocol. In particular, changing the NaOH volume (40μL) and mixing repeats improved gelation. Nonetheless, the problem persisted with the use of new collagen batches. It was apparent, considering that reagent concentrations and volumes did not change the outcome, that the lack of gelation and solution turbidity were signs of collagen denaturation. Although the collagens were acquired from the same, respective sources it was possible that minute changes in preparation could alter the protein environment. This is demonstrated by the minor changes in NaOH volumes for each collagen batch, determined by phenol red titration (not shown). The NaOH volume was insufficient for adjusting the pH, contradicting the pH strip indicators. Furthermore, the total volume injection into the t-piece system immediately damaged the collagen, displayed by localized colouration within the t-joint junction apparent by the sustained turbidity. Therefore, NaOH injections are aliquoted into smaller injections with mixing phases. Finally, the

temperature was closely regulated considering the extended contact with the t-piece system during injection and mixing phases. Overall, the troubleshooting aspect in this project determined that the procedures for rHC hydrogels must be thoroughly examined to ensure high-quality production. To this end, all relevant procedures are now written under SOPs. The final protocol produces quality rHC TI and TIII hydrogels efficiently and consistently.

Intrinsic to biomaterial classification, characterization defines the structural and biological potential of the designed construct. Importantly, the physical, chemical, and mechanical characteristics of the material must meet the requirements of the physiological environment for its application (Boffito et al., 2014, Radhakrishnan et al., 2014). The myocardium is a complex, organized structural and functional system. The post-MI environment destabilizes this system, leaving much to be desired for tissue restoration and replacement (Georgiadis et al., 2014). Therefore, material characteristics must provide an environment that upholds the essential properties distinguished by the healthy, native myocardium. This perspective aims to replicate the unique features of the ECM, which provide support and maintenance to the surrounding cellular environment. Furthermore, local cell populations respond to ECM chemical and biophysical cues in a dynamic, reciprocity that can renew homeostatic integrity (Londono and Badylak, 2015). To this end, both structure and composition contribute to host-material interactions. In particular, collagen-based hydrogels can operate within this application because collagen is integral to the healthy ECM environment (Shapira et al., 2016, Londono and Badylak, 2015). This is crucial, whether hydrogels are intended to encapsulate stem cells for transplantation or modulate myogenic differentiation and communicate with endogenous

stem cells. Most 3D matrices are characterized by their composition, modifications, and altered polymeric structure (Hasan et al., 2015). Therefore, the rHC hydrogels were characterized to demonstrate if their features appropriately endure and support the cardiac environment.

The hydrophilic, water-retentive qualities distinctive to hydrogels appropriately mimic human tissues. In biological systems, cellular and molecular components rely on water for biological processes and structural support. Water swelling/contraction of hydrogels, alike to human tissues, allows them to expand whilst maintaining its original shape (Radhakrishnan et al., 2014). Water is an integral component of collagen and dehydration, even conferred by relatively small changes in surrounding osmotic pressures, can alter collagen conformation (Masic et al., 2015). The effects of dehydration altering collagen conformation affect its functional role too. This is a relatively common problem with decellularized processing for scaffolds, in which the functional activities of ECM-components are diminished after modification (Londono and Badylak, 2015, Hoshiba et al., 2010). Although the rHC hydrogels are cross-linked using a water-soluble carbodiimide, cross-linking density can prevent hydration (Grover et al., 2012, Liu et al., 2006). This interference to post-gelation water retention can have a considerable impact on collagen stability, thus affecting hydrogel performance in biological environments. Generally, water uptake is controlled by composition, porosity, hydrophobicity, and cross-linking density (Davidenko et al., 2010, Liu et al., 2006, Park et al., 2002). Our results for wet to dry water weight comparison determined that the rHC hydrogels have a high water retention capacity (> 93%). It appears that the difference in porosity, discussed below, did not contribute to changes in water uptake. In addition, this

demonstrates the rHC hydrogels maintain structural integrity in the presence of water. Hydrogels resist solubilisation in water because osmotic equilibrium is reached at maximum water retention, or swelling ratio (Asti and Gioglio, 2014, De et al., 2002). However, dissolution in water is affected by cross-linking degree too. This is important, since maximized cross-linkage can alter the mechanical properties, particularly stiffness, of a hydrogel to an extent that renders it unusable for its application. Davidenko *et al.* determined that collagen-based scaffolds with 10-fold diluted (10%) EDC concentration remains stable in water (14 days) compared to scaffolds with maximized (100%) concentration (Davidenko et al., 2015). This demonstrates that cross-linker chemistry for natural materials can be fine-tuned to ensure that hydrogels remain water-insoluble, whilst modifying resistance to other forms of degradation (enzymatic) or mechanical strength and elasticity. In a physiological application, hydrogels should preserve their mechanical properties (stiffness, elasticity) while fully integrating with the fluid environment.

Rheological characteristics define viscoelastic properties in polymeric materials. This is exceptionally useful for soft materials, which are neither fully fluid nor solid state. Specifically, material viscosity is important for injectable materials since aqueous flow during gelation can dictate its feasibility in small (0.5mm) syringe needles or catheter systems. Ideally, the hydrogels should have a low viscosity at high shear rates in this application. The measurements started after gelation, thus the maximum viscosity is the upper-limit for the material within 10 minutes. Therefore, the aqueous hydrogel viscosity is lower than this maximum as it is prepared and/or injected. The viscosity difference between the rHC hydrogels is likely explained by the microstructure properties of the

polymeric networks. The cross-linked fibers differ between the two collagens, thus the intermolecular forces (cross-linked networks) affect the material viscoelastic properties to a different degree. This is most consistent, considering the material concentration (1%; 61% v/v total) and cross-linker concentration (11.7mM; 12% v/v total) were identical for each hydrogel and experiment. McEwan *et al.* demonstrated the rheological differences in EDC/NHS cross-linker concentrations with porcine collagen type I matrices (McEwan et al., 2011). In comparison, the rHC hydrogels have relatable viscosity readings to these collagen matrices using a similar cross-linking procedure. Nonetheless, in the present study, poor reproducibility of the rheology results was encountered. Although hydrogel placement was easy, the compression procedure was difficult. The hydrogels experienced considerable deformation under the spindle, apparent by dry, cracked material within minutes of the measurement. Changes to gap distance and shear rate parameters did not improve this condition. However, the technical problems associated with the experiment are most prevalent with the porcine collagen measurements. The maximum viscosity is quite low compared to the related study (McEwan et al., 2011), and do not correlate to the rest of the Theracol characterization. Furthermore, previous studies used a C50-2/30 (conical) spindle with a larger surface area. This should not affect the porcine collagen variance, but it could resolve the issues affecting the hydrogels placement during the measurements. However, this spindle was not viable at this time with limited sample volumes for rHC TI and TIII. Although hydrogels rapidly gelate after exposure to cross-linker, water retention ensures the material cross-links uniformly. Rheological assessments sometimes incorporate preventative measures to ensure water evaporation is not affected by humidity or physical displacement. In some studies, calibration oils

(Moreno-Arotzena et al., 2015, Wolf et al., 2012) or water humidifiers (Que et al., 2014) are coupled with the sample to negate these complications. In addition, micro-rheology may elucidate viscoelastic properties in hydrogels (aqueous to gel transition) using considerably smaller sample volumes (Que et al., 2014). It is important that these measurements for rheological properties be repeated using the above troubleshooting methods with the current equipment.

Thermal degradation, determined by DSC, is indicative of cross-linking efficiency. Temperature-dependant denaturation affects the conserved, triple helical structure of collagen. This begins to deform the supramolecular structure, resulting in random coil conformations that diminish protein stability (Bozec and Odlyha, 2011). This protein unfolding transition is typically irreversible, which is indicated by a distinct endothermic (negative heat flow) shift as temperature ramping proceeds to a defined maximum. It is from this shift that this transition begins to take effect. Therefore, it is proposed that covalent linkages in collagen can fortify thermal resistance and make the native collagen structure more resistant to denaturation (Grover et al., 2012, Olde Damink et al., 1996). Generally, increased cross-linking degree increases the denaturation temperature, T_D, of biomaterial scaffolds (Angele et al., 2004). Recombinant human and porcine collagens have similar T_D before and after cross-linking at comparable concentrations (Liu et al., 2006, Yang et al., 2004). In our study, the rHC hydrogels' T_D was similar to Theracol, demonstrating that the rHC is as effectively cross-linked by EDC/NHS as animal-derived collagen. In addition, the T_D values are similar to other EDC/NHS cross-linked collagen materials in the literature (Koh et al., 2013, Usha et al., 2012, Liu et al., 2006). Furthermore, the batch-to-batch consistency for the rHC

hydrogels was preserved throughout cross-linking degree. Importantly, this demonstrates the equivalence in preparation and production procedures for the hydrogels. However, the hydrothermal stability of rHC hydrogels was not exceptionally high (> 55% consistently). Nonetheless, this stability is not expected with a low-concentration collagen-only material with mild cross-linking concentration. In effect, collagen materials with higher denaturation temperatures, usually heavily cross-linked dermal patches, often elicit increased pro-inflammatory responses, reduced cell infiltration, and delayed wound healing (Delgado et al., 2015). Overall, the rHC hydrogels are consistently stable beyond physiological temperatures appropriate for their injectable application.

In addition to hydrothermal stability, enzymatic degradation is indicative of cross-linking degree too. In particular, collagens TI, TII, and TIII are susceptible to hydrolysis from MMP-1, MMP-2, MMP-8, MMP-13, and MMP-14, which are enzymes that cleave collagen into fragments for subsequent removal (Chattopadhyay and Raines, 2014, Kahari and Saarialho-Kere, 1997). The intermolecular, covalent bonds from cross-linkers can protect collagen motifs that are susceptible to enzymatic cleavage. This improved resistance is appropriate for materials intended for physiological environments. Furthermore, since cross-linking degree influences enzymatic interactions this can provide a means for controlled scaffold degradation *in-vitro* and *in-vivo*. Collagenase degradation profiles can display differences in hydrogel stability within a biological environment. Importantly, in this experiment MMP-1 (collagenase) induced this degradation. Although collagen TI and TIII are both susceptible to hydrolysis from MMP-1, catalytic activity is higher for collagen TIII depending on the species origin of the collagen (Kahari and Saarialho-Kere, 1997, Welgus et al., 1985). Furthermore, the

helical stability of collagen TIII is suspected to prompt this degradation difference (Welgus et al., 1985). However, the rHC TIII hydrogels in the present study degraded slower in the presence of MMP-1 compared to rHC TI hydrogels. Interestingly, this increased resistance to enzymatic degradation implies that the TIII cross-linking orientation and/or density significantly decreases the accessibility for the enzyme. However, the rHC hydrogels should undergo degradation tests with other enzymes, such as MMP-8, to fully evaluate this conclusion. The concentration of collagenase in this study was considerably greater than other studies, which usually persist over many days instead of hours (Deng et al., 2010, Angele et al., 2004). In studies with identical collagenase concentrations (Koh et al., 2013, Liu et al., 2006), material degradation is considerably slower to our study. However, the material concentrations (> 9% w/w) likely affect degradation rate compared to our 1% hydrogels. This experiment demonstrates that the differences in rHC TI and TIII cross-linking influence enzymatic degradation rates.

EDC/NHS chemistry is not expected to be 100% efficient, and to a degree this is dependent on the availability of substrate (free amine groups) and the concentration of chemical cross-linker. This reaction has provided structure to the hydrogel, yet unreacted reagent remains solubilized. The absorbance profiles for this study indicate that a degree of unreacted EDC/NHS reagent remains in solution after cross-linking is complete. Although, washes quickly remove this excess as the signal begins to disappear. As previously described, EDC is not incorporated in the cross-links and thus material degradation does not affect this detection. Notably, functionalized surface modifications (VEGF, YIGSR / RGD motifs) with carbodiimide chemistry have proven effective for

biomolecule immobilisation without signs of cytotoxicity or significant inflammation (Shapira et al., 2016, Tallawi et al., 2015). In our study, fibroblast cell cultures seeded onto rHC hydrogels did not display limited growth or abnormal physical features. The chemical by-products in our procedure do not appear to inhibit cell growth. Cell media changes, although infrequent, for the *in-vitro* experiments are representative of the washes in this absorbance experiment. *In-vivo*, it is expected that the body's circulation will remove unreacted components of the hydrogel, and as shown by our lab (Blackburn et al., 2015, Kuraitis et al., 2013), the diluted by-products of injectable materials using EDC/NHS chemistry do not pose a toxicity risk. However, quantified analysis of cytotoxic or pro-inflammatory indicators should be subject to the rHC hydrogels with seeded fibroblasts or cardiac endothelial cells. This can ensure that the chemical cross-linker, or the cross-linking degree, is appropriate for injectable applications.

For a biomaterial to mimic the ECM microenvironment, the external and internal physical structure should promote material-cellular interactions. In particular, the biophysical cues intrinsic to the 3D structure of collagen-based hydrogels are important to scaffold performance. Importantly, surface topography and porosity influence cell behaviours by modulating adhesion, morphology, migration, alignment, and distribution (Zhang et al., 2015a, Wang et al., 2011). Furthermore, porosity and pore interconnectivity improve cell survival, whilst allowing cell ingrowth and nutrient diffusion necessary for high cell viability (Zhang et al., 2015a, Annabi et al., 2010). In effect, microporous networks provide an ECM microarchitecture that facilitates cell permeability. This surface area and porosity density interplay is maximized by hydrogel structural configuration in physiological environments. The rHC TI hydrogels have a high density

of small pores (H: 9.5 ± 0.3μm / W: 10.5 ± 0.4μm) organized in layered sheets. In contrast, rHC TIII hydrogels have larger, clustered pores (H: 27.3 ± 1.0μm / W: 24.2 ± 0.9μm) that appear globular and swollen. This considerable difference in pore dimensions and interconnectivity indicates that the cross-linking, with the same concentration, creates different porous networks based on the collagen type. In addition, microarchitecture differs depending on the source of collagen, which was reported in bovine collagens from different tissue extracts (Davidenko et al., 2015). This is apparent when the rHC hydrogels are compared to the microporous architecture of Theracol. Although the differences in pore dimensions of Theracol to rHC TI are not striking, the landscape pattern differs, as seen in the SEM images. The uniform porosity of rHC TI hydrogels is potentially beneficial for material contractions and ECM secretion. The larger pore dimensions in rHC TIII may provide a more spacious environment for cell migration and ingrowth. However, optimal porosity for fibroblast growth in hydrogel matrices is approximately 5-15μm (Annabi et al., 2010). Porosity measurements are not absolutes, considering that hydrogel 3D environment is layered with internal channels that intercalate the entire matrix. Nonetheless, these identified differences in rHC microarchitectures are essential for future interpretations on hydrogel structural and functional performance.

Collagen-based matrices are anticipated to interact with the cellular environment and surrounding tissues as a support scaffold. Therefore, to understand the suitability of rHC hydrogels in a physiological environment, the cytocompatibility was evaluated using mouse cardiac fibroblasts. Fibroblasts were used for two reasons: 1) they proliferate rapidly, providing a good read-out for cytocompatibility, and 2) they are a relevant cell

type in the remodeling post-MI cardiac ECM. Furthermore, cardiac fibroblasts are ideal because of the role they play in cardiac healing and scar formation after an MI (Radhakrishnan et al., 2014, Fan et al., 2012). The morphology and proliferation of cardiac fibroblasts grown in the presence of rHC hydrogels was evaluated in comparison to a control plate of TCPS over a 5-day period. Cardiac fibroblast growth was observed in all conditions, with differences in cellular alignment and orientation. In particular, rHC hydrogel fibroblasts were located on the material surface and within the interior of the hydrogel after cultures were established. This complements the porosity analysis, indicating that the pore sizes for both rHC hydrogels are sufficient for cell infiltration. However, the multi-layered growth can be explored further by cross-section staining for fibroblast indicators with microscopy to ascertain the % interior cell population. At the time of the experiments, the microscope lens was displaced. This resulting interference disrupted the image quality, and repairs were not complete until late in the project.

Cell staining improved visualization of healthy fibroblast morphology on rHC hydrogels. For a pre-confluent culture, there was no indication of mass apoptosis, membrane shrinkage, or impaired cytoskeleton extensions for rHC hydrogels. In addition, hydrogels were uncompromised throughout the 5-day period. Proliferative analysis indicates that both rHC TI and TIII support cell growth and mediate cellular expansion. The EDC/NHS cross-linker could explain the minimal fibroblast proliferation on rHC TI and TIII hydrogels on day 1. Concentration-dependent EDC collagen materials affect fibroblast viability (Saito et al., 2008), although the extent of cytotoxicity in this study was not observed in our results. Presumably, despite the early differences, the effects were not long-lasting since cell growth was unhindered throughout the other later time-

points. However, the observed biocompatibility of the rHC hydrogels is important for future design applications in human translational medicine. Techniques to fabricate full-length, hydroxylated rHC are beginning to arise in the literature (Que et al., 2014). The means to more efficiently produce rHC or modify variant sequences with site-specific precision can open many doors for TERM biomaterial design. Furthermore, biosynthesis of recombinant human proteins will ultimately reach supply demands without batch-to-batch variability and manufacturer difficulties. These complications are apparent in other attempts for human-based scaffolds, such as decellularized human myocardial matrices (Johnson et al., 2014). Therefore, the biocompatibility of rHC TI and TIII hydrogels *in-vitro* prompts further exploration of the hydrogel impact on cell behaviour, and *in-vivo* performance.

4.2 Future Directions

There are a few limitations to this study, although limited rHC TI supply was a major obstacle for project progression. Unfortunately, the expense currently associated with full-scale rHC products is an issue. The cost per gram of rHC is exceedingly high with a low yield compared to animal-derived collagens (Liu et al., 2013, Baez et al., 2005). The costs are reduced with minimized use of collagen, such as surface coatings, electrospun fibers, or low collagen percentage mixtures. The high cost of rHC TI limited the number of *in-vitro* investigations that could be performed. To address this, thinner hydrogel plate coatings may be an option to minimize rHC use in the future. This minimalistic approach should be implemented at the start of the experiment, to avoid shortages after necessary calibrations or troubleshooting with cell models. In the future,

the demand for such biosynthetic materials will likely propagate commercialization and lower expenses especially with new methods in recombinant bacterial collagen (An et al., 2014). Nonetheless, rHC offers a safe, modifiable, and consistent alternative to natural, animal-derived collagens.

Furthermore, there are other routes available for improvement. The rheological characteristics should be ascertained, but other material properties of interest could be investigated too. In terms of mechanical characterization, rHC hydrogel stress/strain curves and elastic moduli can be used to interpret material stiffness and compression resistance. Furthermore, the water content analysis can be enhanced with long-term swelling ratio experiments in water, cell media, and myocardial matrix. Degradation experiments could benefit from lower concentrations of collagenase, which allow long-term (> 2 weeks) dissolution and degradation analysis. The hydrogels are highly hydrophilic, and water contact angle measurements could identify physical differences between the cross-linked polymeric rHC hydrogel surfaces. In addition, individual fibers should be visualized by cryo-SEM at a greater magnification (~10-50μm scale). Although EDC/NHS cross-linking was effective with the rHC hydrogels, quantitative measures for free amine groups ($-NH_2$) before and after cross-linking using 2,4,6-trinitrobenzene sulfonic acid could be beneficial to the study (Bubnis and Ofner, 1992). Although studies referred herein establish that at our EDC/NHS concentration and molar ratio, the number of reacted amines are 25-28 groups / 1000 residues (~2.0-3.0%), from literature source amine content being ~30 groups / 1000 residues (Pieper et al., 2000, Liu et al., 2006, Yang, 2012). Nonetheless, distinct differences in material source and cross-linker concentration/ratio should prompt this investigation. This study demonstrates the *in vitro*

cytocompatibility of the rHC hydrogels. In addition, compatibility experiments should investigate cell survival and growth using live/dead assays and gene expression changes could be examined over a 5-day period. Furthermore, experiments on cardiac endothelial cells and/or stem/progenitor cells will complement this study on cell behaviour with rHC hydrogels. Once the appropriate material is prepared, it will be tested in acute MI models using small animals (mice) and large animals (pigs). Primary end-points for this evaluation of the injectable hydrogel will be regenerative potency and heart performance. Hydrogel injections into animals should not elicit an immunogenic and thrombogenic response in long-term assessments. Subsequent measures on cardiac output, end-systolic, end-diastolic, and ejection fraction indicators, will determine cardiac function and the hydrogel's repair/healing efficacy. In addition, comparative measures of scar area thickness and infarct tissue mechanical properties in the presence of rHC hydrogels should complement performance analysis. The overall rHC hydrogel performance in promoting cardiac muscle angiogenesis and neovascularization in animal models should display improvement in regeneration. To this end, it is anticipated that the rHC TI or TIII injectable hydrogels can provide sufficient replacement of scarred tissue that could reverse LV dilation, adverse remodeling, and possibly promote myocardial regeneration.

5 Chapter: Conclusions

Although natural-based TERM biomaterials for post-MI repair and regeneration are steadily under investigation, their application in cardiac treatment is delayed by numerous challenges. The exact mechanisms driving hydrogel regenerative benefits are not understood, nor are the parameters best associated with improved cardiac function. Nonetheless, this knowledge gap will surely close in time with rapid advancement in revolutionary biomaterial engineering. Progress towards novel, clinically relevant materials will hasten this momentum and development will readily follow pre-clinical investigation. Therefore, this study builds upon these concepts and demonstrates the potential application of recombinant human collagen TI and TIII injectable hydrogels. To our knowledge, this is the first human source collagen biomaterial developed for cardiac regeneration. Overall, this work characterizes the physical, chemical, and cytocompatibility properties of rHC hydrogels and contributes to our understanding of rHC biomaterials. It is anticipated that future work on these recombinant human collagen hydrogels will accelerate the development of engineered, biofunctional materials for cardiac regenerative therapy.

Bibliography

AHMADI, A., MCNEILL, B., VULESEVIC, B., KORDOS, M., MESANA, L., THORN, S., RENAUD, J. M., MANTHORP, E., KURAITIS, D., TOEG, H., MESANA, T. G., DAVIS, D. R., BEANLANDS, R. S., DASILVA, J. N., DEKEMP, R. A., RUEL, M. & SUURONEN, E. J. 2014. The role of integrin alpha2 in cell and matrix therapy that improves perfusion, viability and function of infarcted myocardium. *Biomaterials,* 35**,** 4749-58.

AN, B., KAPLAN, D. L. & BRODSKY, B. 2014. Engineered recombinant bacterial collagen as an alternative collagen-based biomaterial for tissue engineering. *Front Chem,* 2**,** 40.

ANGELE, P., ABKE, J., KUJAT, R., FALTERMEIER, H., SCHUMANN, D., NERLICH, M., KINNER, B., ENGLERT, C., RUSZCZAK, Z., MEHRL, R. & MUELLER, R. 2004. Influence of different collagen species on physico-chemical properties of crosslinked collagen matrices. *Biomaterials,* 25**,** 2831-41.

ANNABI, N., NICHOL, J. W., ZHONG, X., JI, C., KOSHY, S., KHADEMHOSSEINI, A. & DEHGHANI, F. 2010. Controlling the porosity and microarchitecture of hydrogels for tissue engineering. *Tissue Eng Part B Rev,* 16**,** 371-83.

ASTI, A. & GIOGLIO, L. 2014. Natural and synthetic biodegradable polymers: different scaffolds for cell expansion and tissue formation. *Int J Artif Organs,* 37**,** 187-205.

BAEZ, J., OLSEN, D. & POLAREK, J. W. 2005. Recombinant microbial systems for the production of human collagen and gelatin. *Appl Microbiol Biotechnol,* 69**,** 245-52.

BLACKBURN, N. J., SOFRENOVIC, T., KURAITIS, D., AHMADI, A., MCNEILL, B., DENG, C., RAYNER, K. J., ZHONG, Z., RUEL, M. & SUURONEN, E. J. 2015. Timing underpins the benefits associated with injectable collagen biomaterial therapy for the treatment of myocardial infarction. *Biomaterials,* 39**,** 182-92.

BOFFITO, M., SARTORI, S. & CIARDELLI, G. 2014. Polymeric scaffolds for cardiac tissue engineering: requirements and fabrication technologies. *Polym Int,* 63**,** 2-11.

BOZEC, L. & ODLYHA, M. 2011. Thermal denaturation studies of collagen by microthermal analysis and atomic force microscopy. *Biophys J,* 101**,** 228-36.

BUBNIS, W. A. & OFNER, C. M., 3RD 1992. The determination of epsilon-amino groups in soluble and poorly soluble proteinaceous materials by a spectrophotometric method using trinitrobenzenesulfonic acid. *Anal Biochem,* 207**,** 129-33.

CAO, H. & XU, S. Y. 2008. EDC/NHS-crosslinked type II collagen-chondroitin sulfate scaffold: characterization and in vitro evaluation. *J Mater Sci Mater Med,* 19**,** 567-75.

CAULFIELD, J. B. & JANICKI, J. S. 1997. Structure and function of myocardial fibrillar collagen. *Technol Health Care,* 5**,** 95-113.

CHACHQUES, J. C., PRADAS, M. M., BAYES-GENIS, A. & SEMINO, C. 2013. Creating the bioartificial myocardium for cardiac repair: challenges and clinical targets. *Expert Rev Cardiovasc Ther,* 11**,** 1701-11.

CHACHQUES, J. C., TRAININI, J. C., LAGO, N., CORTES-MORICHETTI, M., SCHUSSLER, O. & CARPENTIER, A. 2008. Myocardial Assistance by Grafting a New Bioartificial Upgraded Myocardium (MAGNUM trial): clinical feasibility study. *Ann Thorac Surg,* 85**,** 901-8.

CHATTOPADHYAY, S. & RAINES, R. T. 2014. Review collagen-based biomaterials for wound healing. *Biopolymers,* 101**,** 821-33.

CHRISTMAN, K. L., FOK, H. H., SIEVERS, R. E., FANG, Q. & LEE, R. J. 2004. Fibrin glue alone and skeletal myoblasts in a fibrin scaffold preserve cardiac function after myocardial infarction. *Tissue Eng,* 10**,** 403-9.

D'AMORE, A., YOSHIZUMI, T., LUKETICH, S. K., WOLF, M. T., GU, X., CAMMARATA, M., HOFF, R., BADYLAK, S. F. & WAGNER, W. R. 2016. Bi-layered polyurethane - Extracellular matrix cardiac patch improves ischemic ventricular wall remodeling in a rat model. *Biomaterials,* 107**,** 1-14.

DAI, W., HALE, S. L., KAY, G. L., JYRALA, A. J. & KLONER, R. A. 2009. Delivering stem cells to the heart in a collagen matrix reduces relocation of cells to other organs as assessed by nanoparticle technology. *Regen Med,* 4**,** 387-95.

DAVIDENKO, N., CAMPBELL, J. J., THIAN, E. S., WATSON, C. J. & CAMERON, R. E. 2010. Collagen-hyaluronic acid scaffolds for adipose tissue engineering. *Acta Biomater,* 6**,** 3957-68.

DAVIDENKO, N., SCHUSTER, C. F., BAX, D. V., RAYNAL, N., FARNDALE, R. W., BEST, S. M. & CAMERON, R. E. 2015. Control of crosslinking for tailoring collagen-based scaffolds stability and mechanics. *Acta Biomater,* 25**,** 131-42.

DE, S. K., ALURU, N. R., JOHNSON, B., CRONE, W. C., BEEBE, D. J. & MOORE, J. 2002. Equilibrium swelling and kinetics of pH-responsive hydrogels: Models, experiments, and simulations. *J Microelectromech Syst,* 11**,** 544-555.

DELGADO, L. M., BAYON, Y., PANDIT, A. & ZEUGOLIS, D. I. 2015. To cross-link or not to cross-link? Cross-linking associated foreign body response of collagen-based devices. *Tissue Eng Part B Rev,* 21**,** 298-313.

DENG, C., ZHANG, P., VULESEVIC, B., KURAITIS, D., LI, F., YANG, A. F., GRIFFITH, M., RUEL, M. & SUURONEN, E. J. 2010. A collagen-chitosan hydrogel for endothelial differentiation and angiogenesis. *Tissue Eng Part A,* 16**,** 3099-109.

DISTEFANO, G. & SCIACCA, P. 2012. Molecular pathogenesis of myocardial remodeling and new potential therapeutic targets in chronic heart failure. *Ital J Pediatr,* 38**,** 41.

DUAN, Y., LIU, Z., O'NEILL, J., WAN, L. Q., FREYTES, D. O. & VUNJAK-NOVAKOVIC, G. 2011. Hybrid gel composed of native heart matrix and collagen induces cardiac differentiation of human embryonic stem cells without supplemental growth factors. *J Cardiovasc Transl Res,* 4**,** 605-15.

ENGEL, J. & PROCKOP, D. J. 1991. The zipper-like folding of collagen triple helices and the effects of mutations that disrupt the zipper. *Annu Rev Biophys Biophys Chem,* 20**,** 137-52.

EPELMAN, S., LIU, P. P. & MANN, D. L. 2015. Role of innate and adaptive immune mechanisms in cardiac injury and repair. *Nat Rev Immunol,* 15**,** 117-29.

FAGERHOLM, P., LAGALI, N. S., MERRETT, K., JACKSON, W. B., MUNGER, R., LIU, Y., POLAREK, J. W., SODERQVIST, M. & GRIFFITH, M. 2010. A

biosynthetic alternative to human donor tissue for inducing corneal regeneration: 24-month follow-up of a phase 1 clinical study. *Sci Transl Med,* 2**,** 46ra61.
FAGERHOLM, P., LAGALI, N. S., ONG, J. A., MERRETT, K., JACKSON, W. B., POLAREK, J. W., SUURONEN, E. J., LIU, Y., BRUNETTE, I. & GRIFFITH, M. 2014. Stable corneal regeneration four years after implantation of a cell-free recombinant human collagen scaffold. *Biomaterials,* 35**,** 2420-7.
FAN, D., TAKAWALE, A., LEE, J. & KASSIRI, Z. 2012. Cardiac fibroblasts, fibrosis and extracellular matrix remodeling in heart disease. *Fibrogenesis Tissue Repair,* 5**,** 15.
FICHARD, A., TILLET, E., DELACOUX, F., GARRONE, R. & RUGGIERO, F. 1997. Human recombinant alpha1(V) collagen chain. Homotrimeric assembly and subsequent processing. *J Biol Chem,* 272**,** 30083-7.
FINOSH, G. T. & JAYABALAN, M. 2012. Regenerative therapy and tissue engineering for the treatment of end-stage cardiac failure: new developments and challenges. *Biomatter,* 2**,** 1-14.
FRANGOGIANNIS, N. G. 2014. The inflammatory response in myocardial injury, repair, and remodelling. *Nat Rev Cardiol,* 11**,** 255-65.
GALVEZ-MONTON, C., PRAT-VIDAL, C., ROURA, S., SOLER-BOTIJA, C. & BAYES-GENIS, A. 2013. Update: Innovation in cardiology (IV). Cardiac tissue engineering and the bioartificial heart. *Rev Esp Cardiol (Engl Ed),* 66**,** 391-9.
GARBERN, J. C. & LEE, R. T. 2013. Cardiac stem cell therapy and the promise of heart regeneration. *Cell Stem Cell,* 12**,** 689-98.
GASIOROWSKI, J. Z., MURPHY, C. J. & NEALEY, P. F. 2013. Biophysical cues and cell behavior: the big impact of little things. *Annu Rev Biomed Eng,* 15**,** 155-76.
GAZOTI DEBESSA, C. R., MESIANO MAIFRINO, L. B. & RODRIGUES DE SOUZA, R. 2001. Age related changes of the collagen network of the human heart. *Mech Ageing Dev,* 122**,** 1049-58.
GEORGIADIS, V., KNIGHT, R. A., JAYASINGHE, S. N. & STEPHANOU, A. 2014. Cardiac tissue engineering: renewing the arsenal for the battle against heart disease. *Integr Biol (Camb),* 6**,** 111-26.
GROVER, C. N., CAMERON, R. E. & BEST, S. M. 2012. Investigating the morphological, mechanical and degradation properties of scaffolds comprising collagen, gelatin and elastin for use in soft tissue engineering. *J Mech Behav Biomed Mater,* 10**,** 62-74.
HANEEF, K., LILA, N., BENADDA, S., LEGRAND, F., CARPENTIER, A. & CHACHQUES, J. C. 2012. Development of bioartificial myocardium by electrostimulation of 3D collagen scaffolds seeded with stem cells. *Heart Int,* 7**,** e14.
HASAN, A., KHATTAB, A., ISLAM, M. A., HWEIJ, K. A., ZEITOUNY, J., WATERS, R., SAYEGH, M., HOSSAIN, M. M. & PAUL, A. 2015. Injectable Hydrogels for Cardiac Tissue Repair after Myocardial Infarction. *Adv Sci (Weinh),* 2**,** 1500122.
HENKEL, W. & GLANVILLE, R. W. 1982. Covalent crosslinking between molecules of type I and type III collagen. The involvement of the N-terminal, nonhelical regions of the alpha 1 (I) and alpha 1 (III) chains in the formation of intermolecular crosslinks. *Eur J Biochem,* 122**,** 205-13.

HEYDARKHAN-HAGVALL, S., SCHENKE-LAYLAND, K., DHANASOPON, A. P., ROFAIL, F., SMITH, H., WU, B. M., SHEMIN, R., BEYGUI, R. E. & MACLELLAN, W. R. 2008. Three-dimensional electrospun ECM-based hybrid scaffolds for cardiovascular tissue engineering. *Biomaterials,* 29**,** 2907-14.

HILFIKER-KLEMER, D. L., U. DREXLER, H. 2006. Molecular mechanisms in heart failure - Focus on cardiac hypertrophy, inflammation, angiogenesis, and apoptosis. *J Am Coll Cardiol,* 48**,** A56-66.

HOSHIBA, T., LU, H., KAWAZOE, N. & CHEN, G. 2010. Decellularized matrices for tissue engineering. *Expert Opin Biol Ther,* 10**,** 1717-28.

HWANG, E. S., THIAGARAJAN, G., PARMAR, A. S. & BRODSKY, B. 2010. Interruptions in the collagen repeating tripeptide pattern can promote supramolecular association. *Protein Sci,* 19**,** 1053-64.

JOHNSON, T. D. & CHRISTMAN, K. L. 2013. Injectable hydrogel therapies and their delivery strategies for treating myocardial infarction. *Expert Opin Drug Deliv,* 10**,** 59-72.

JOHNSON, T. D., DEQUACH, J. A., GAETANI, R., UNGERLEIDER, J., ELHAG, D., NIGAM, V., BEHFAR, A. & CHRISTMAN, K. L. 2014. Human versus porcine tissue sourcing for an injectable myocardial matrix hydrogel. *Biomater Sci,* 2014**,** 60283D.

KAHARI, V. M. & SAARIALHO-KERE, U. 1997. Matrix metalloproteinases in skin. *Exp Dermatol,* 6**,** 199-213.

KOH, L. B., ISLAM, M. M., MITRA, D., NOEL, C. W., MERRETT, K., ODORCIC, S., FAGERHOLM, P., JACKSON, W. B., LIEDBERG, B., PHOPASE, J. & GRIFFITH, M. 2013. Epoxy cross-linked collagen and collagen-laminin Peptide hydrogels as corneal substitutes. *J Funct Biomater,* 4**,** 162-77.

KURAITIS, D., BERARDINELLI, M. G., SUURONEN, E. J. & MUSARO, A. 2013. A necrotic stimulus is required to maximize matrix-mediated myogenesis in mice. *Dis Model Mech,* 6**,** 793-801.

KURAITIS, D., EBADI, D., ZHANG, P., RIZZUTO, E., VULESEVIC, B., PADAVAN, D. T., AL MADHOUN, A., MCEWAN, K. A., SOFRENOVIC, T., NICHOLSON, K., WHITMAN, S. C., MESANA, T. G., SKERJANC, I. S., MUSARO, A., RUEL, M. & SUURONEN, E. J. 2012a. Injected matrix stimulates myogenesis and regeneration of mouse skeletal muscle after ischaemic injury. *Eur Cell Mater,* 24**,** 175-95; discussion 195-6.

KURAITIS, D., GIORDANO, C., RUEL, M., MUSARO, A. & SUURONEN, E. J. 2012b. Exploiting extracellular matrix-stem cell interactions: a review of natural materials for therapeutic muscle regeneration. *Biomaterials,* 33**,** 428-43.

KURAITIS, D., SUURONEN, E. J., SELLKE, F. W. & RUEL, M. 2010. The future of regenerating the myocardium. *Curr Opin Cardiol,* 25**,** 575-82.

LAM, M. T. & WU, J. C. 2012. Biomaterial applications in cardiovascular tissue repair and regeneration. *Expert Rev Cardiovasc Ther,* 10**,** 1039-49.

LEE, K., SILVA, E. A. & MOONEY, D. J. 2011. Growth factor delivery-based tissue engineering: general approaches and a review of recent developments. *J R Soc Interface,* 8**,** 153-70.

LIU, W., BURDICK, J. A. & VAN OSCH, G. J. 2013. Plant-derived recombinant human collagen: a strategic approach for generating safe human ECM-based scaffold. *Tissue Eng Part A,* 19**,** 1489-90.

LIU, X., WU, H., BYRNE, M., KRANE, S. & JAENISCH, R. 1997. Type III collagen is crucial for collagen I fibrillogenesis and for normal cardiovascular development. *Proc Natl Acad Sci U S A,* 94**,** 1852-6.

LIU, Y., GRIFFITH, M., WATSKY, M. A., FORRESTER, J. V., KUFFOVA, L., GRANT, D., MERRETT, K. & CARLSSON, D. J. 2006. Properties of porcine and recombinant human collagen matrices for optically clear tissue engineering applications. *Biomacromolecules,* 7**,** 1819-28.

LIU, Y., XU, Y., WANG, Z., WEN, D., ZHANG, W., SCHMULL, S., LI, H., CHEN, Y. & XUE, S. 2016. Electrospun nanofibrous sheets of collagen/elastin/polycaprolactone improve cardiac repair after myocardial infarction. *Am J Transl Res,* 8**,** 1678-94.

LONDONO, R. & BADYLAK, S. F. 2015. Biologic scaffolds for regenerative medicine: mechanisms of in vivo remodeling. *Ann Biomed Eng,* 43**,** 577-92.

LOPEZ SALAZAR, B., RAVASSA ALBENIZ, S., ARIAS GUEDON, T., GONZALEZ MIQUEO, A., QUEREJETA, R. & DIEZ MARTINEZ, J. 2006. [Altered fibrillar collagen metabolism in hypertensive heart failure. Current understanding and future prospects]. *Rev Esp Cardiol,* 59**,** 1047-57.

MARIJIANOWSKI, M. M., TEELING, P., MANN, J. & BECKER, A. E. 1995. Dilated cardiomyopathy is associated with an increase in the type I/type III collagen ratio: a quantitative assessment. *J Am Coll Cardiol,* 25**,** 1263-72.

MARTINEZ-RAMOS, C., RODRIGUEZ-PEREZ, E., GARNES, M. P., CHACHQUES, J. C., MORATAL, D., VALLES-LLUCH, A. & MONLEON PRADAS, M. 2014. Design and assembly procedures for large-sized biohybrid scaffolds as patches for myocardial infarct. *Tissue Eng Part C Methods,* 20**,** 817-27.

MASIC, A., BERTINETTI, L., SCHUETZ, R., CHANG, S. W., METZGER, T. H., BUEHLER, M. J. & FRATZL, P. 2015. Osmotic pressure induced tensile forces in tendon collagen. *Nat Commun,* 6**,** 5942.

MAYFIELD, A. E., TILOKEE, E. L., LATHAM, N., MCNEILL, B., LAM, B. K., RUEL, M., SUURONEN, E. J., COURTMAN, D. W., STEWART, D. J. & DAVIS, D. R. 2014. The effect of encapsulation of cardiac stem cells within matrix-enriched hydrogel capsules on cell survival, post-ischemic cell retention and cardiac function. *Biomaterials,* 35**,** 133-42.

MCEWAN, K., PADAVAN, D. T., DENG, C., VULESEVIC, B., KURAITIS, D., KORBUTT, G. S. & SUURONEN, E. J. 2011. Tunable Collagen Hydrogels are Modified by the Therapeutic Agents They are Designed to Deliver. *J Biomater Sci Polym Ed*.

MORENO-AROTZENA, O., MEIER, J. G., DEL AMO, C. & GARCIA-AZNAR, J. M. 2015. Characterization of Fibrin and Collagen Gels for Engineering Wound Healing Models. *Materials (Basel),* 8**,** 1636-1651.

MOZAFFARIAN, D., BENJAMIN, E. J., GO, A. S., ARNETT, D. K., BLAHA, M. J., CUSHMAN, M., DE FERRANTI, S., DESPRES, J., FULLERTON, H. J., HOWARD, V. J., HUFFMAN, M. D., JUDD, S. E., KISSELA, B. M., LACKLAND, D. T., LICHTMAN, J. H., LISABETH, L. D., LIU, S., MACKEY,

R. H., MATCHAR, D. B., MCGUIRE, D. K., MOHLER, E. R., 3RD, MOY, C. S., MUNTNER, P., MUSSOLINO, M. E., NASIR, K., NEUMAR, R. W., NICHOL, G., PALANIAPPAN, L., PANDEY, D. K., REEVES, M. J., RODRIGUEZ, C. J., SORLIE, P. D., STEIN, J., TOWFIGHI, A., TURAN, T. N., VIRANI, S. S., WILLEY, J. Z., WOO, D., YEH, R. W. & TURNER, M. B. 2014. Heart Disease and Stroke Statistics-2015 Update: A Report From the American Heart Association. *Circulation*.

MUEHLEDER, S., OVSIANIKOV, A., ZIPPERLE, J., REDL, H. & HOLNTHONER, W. 2014. Connections matter: channeled hydrogels to improve vascularization. *Front Bioeng Biotechnol,* 2**,** 52.

MUHONEN, V., SALONIUS, E., HAAPARANTA, A. M., JARVINEN, E., PAATELA, T., MELLER, A., HANNULA, M., BJORKMAN, M., PYHALTO, T., ELLA, V., VASARA, A., TOYRAS, J., KELLOMAKI, M. & KIVIRANTA, I. 2016. Articular cartilage repair with recombinant human type II collagen/polylactide scaffold in a preliminary porcine study. *J Orthop Res,* 34**,** 745-53.

MURRY, C. E., REINECKE, H. & PABON, L. M. 2006. Regeneration gaps: observations on stem cells and cardiac repair. *J Am Coll Cardiol,* 47**,** 1777-85.

NUNES, S. S., MIKLAS, J. W., LIU, J., ASCHAR-SOBBI, R., XIAO, Y., ZHANG, B., JIANG, J., MASSE, S., GAGLIARDI, M., HSIEH, A., THAVANDIRAN, N., LAFLAMME, M. A., NANTHAKUMAR, K., GROSS, G. J., BACKX, P. H., KELLER, G. & RADISIC, M. 2013. Biowire: a platform for maturation of human pluripotent stem cell-derived cardiomyocytes. *Nat Methods,* 10**,** 781-7.

NUUTILA, K., PEURA, M., SUOMELA, S., HUKKANEN, M., SILTANEN, A., HARJULA, A., VUOLA, J. & KANKURI, E. 2015. Recombinant human collagen III gel for transplantation of autologous skin cells in porcine full-thickness wounds. *J Tissue Eng Regen Med,* 9**,** 1386-93.

OGLE, B. M., BURSAC, N., DOMIAN, I., HUANG, N. F., MENASCHE, P., MURRY, C. E., PRUITT, B., RADISIC, M., WU, J. C., WU, S. M., ZHANG, J., ZIMMERMANN, W. H. & VUNJAK-NOVAKOVIC, G. 2016. Distilling complexity to advance cardiac tissue engineering. *Sci Transl Med,* 8**,** 342ps13.

OLDE DAMINK, L. H., DIJKSTRA, P. J., VAN LUYN, M. J., VAN WACHEM, P. B., NIEUWENHUIS, P. & FEIJEN, J. 1996. Cross-linking of dermal sheep collagen using a water-soluble carbodiimide. *Biomaterials,* 17**,** 765-73.

ORZA, A., SORITAU, O., OLENIC, L., DIUDEA, M., FLOREA, A., RUS CIUCA, D., MIHU, C., CASCIANO, D. & BIRIS, A. S. 2011. Electrically conductive gold-coated collagen nanofibers for placental-derived mesenchymal stem cells enhanced differentiation and proliferation. *ACS Nano,* 5**,** 4490-503.

PARENTEAU-BAREIL, R., GAUVIN, R. & BERTHOD, F. 2010. Collagen-Based Biomaterials for Tissue Engineering Applications. *Materials,* 3**,** 1863-1887.

PARK, H., RADISIC, M., LIM, J. O., CHANG, B. H. & VUNJAK-NOVAKOVIC, G. 2005. A novel composite scaffold for cardiac tissue engineering. *In Vitro Cell Dev Biol Anim,* 41**,** 188-96.

PARK, S. N., PARK, J. C., KIM, H. O., SONG, M. J. & SUH, H. 2002. Characterization of porous collagen/hyaluronic acid scaffold modified by 1-ethyl-3-(3-dimethylaminopropyl)carbodiimide cross-linking. *Biomaterials,* 23**,** 1205-12.

PAUSCHINGER, M., KNOPF, D., PETSCHAUER, S., DOERNER, A., POLLER, W., SCHWIMMBECK, P. L., KUHL, U. & SCHULTHEISS, H. P. 1999. Dilated cardiomyopathy is associated with significant changes in collagen type I/III ratio. *Circulation,* 99**,** 2750-6.

PEREA-GIL, I., PRAT-VIDAL, C. & BAYES-GENIS, A. 2015. In vivo experience with natural scaffolds for myocardial infarction: the times they are a-changin'. *Stem Cell Res Ther,* 6**,** 248.

PIEPER, J. S., HAFMANS, T., VEERKAMP, J. H. & VAN KUPPEVELT, T. H. 2000. Development of tailor-made collagen-glycosaminoglycan matrices: EDC/NHS crosslinking, and ultrastructural aspects. *Biomaterials,* 21**,** 581-93.

PRABHAKARAN, M. P., MOBARAKEH, L. G., KAI, D., KARBALAIE, K., NASR-ESFAHANI, M. H. & RAMAKRISHNA, S. 2014. Differentiation of embryonic stem cells to cardiomyocytes on electrospun nanofibrous substrates. *J Biomed Mater Res B Appl Biomater,* 102**,** 447-54.

PRABHAKARAN, M. P., NAIR, A. S., KAI, D. & RAMAKRISHNA, S. 2012. Electrospun composite scaffolds containing poly(octanediol-co-citrate) for cardiac tissue engineering. *Biopolymers,* 97**,** 529-38.

QUE, R., MOHRAZ, A., DA SILVA, N. A. & WANG, S. W. 2014. Expanding functionality of recombinant human collagen through engineered non-native cysteines. *Biomacromolecules,* 15**,** 3540-9.

RADHAKRISHNAN, J., KRISHNAN, U. M. & SETHURAMAN, S. 2014. Hydrogel based injectable scaffolds for cardiac tissue regeneration. *Biotechnol Adv,* 32**,** 449-61.

RANE, A. A. & CHRISTMAN, K. L. 2011. Biomaterials for the treatment of myocardial infarction: a 5-year update. *J Am Coll Cardiol,* 58**,** 2615-29.

RAO, S. V., ZEYMER, U., DOUGLAS, P. S., AL-KHALIDI, H., LIU, J., GIBSON, C. M., HARRISON, R. W., JOSEPH, D. S., HEYRMAN, R. & KRUCOFF, M. W. 2015. A randomized, double-blind, placebo-controlled trial to evaluate the safety and effectiveness of intracoronary application of a novel bioabsorbable cardiac matrix for the prevention of ventricular remodeling after large ST-segment elevation myocardial infarction: Rationale and design of the PRESERVATION I trial. *Am Heart J,* 170**,** 929-37.

RAO, S. V., ZEYMER, U., DOUGLAS, P. S., AL-KHALIDI, H., WHITE, J. A., LIU, J., LEVY, H., GUETTA, V., GIBSON, C. M., TANGUAY, J. F., VERMEERSCH, P., RONCALLI, J., KASPRZAK, J. D., HENRY, T. D., FREY, N., KRACOFF, O., TRAVERSE, J. H., CHEW, D. P., LOPEZ-SENDON, J., HEYRMAN, R. & KRUCOFF, M. W. 2016. Bioabsorbable Intracoronary Matrix for Prevention of Ventricular Remodeling After Myocardial Infarction. *J Am Coll Cardiol,* 68**,** 715-23.

SAITO, H., MURABAYASHI, S., MITAMURA, Y. & TAGUCHI, T. 2008. Characterization of alkali-treated collagen gels prepared by different crosslinkers. *J Mater Sci Mater Med,* 19**,** 1297-305.

SANGANALMATH, S. K. & BOLLI, R. 2013. Cell therapy for heart failure: a comprehensive overview of experimental and clinical studies, current challenges, and future directions. *Circ Res,* 113**,** 810-34.

SCHUSSLER, O., CHACHQUES, J. C., MESANA, T. G., SUURONEN, E. J., LECARPENTIER, Y. & RUEL, M. 2010. 3-dimensional structures to enhance cell therapy and engineer contractile tissue. *Asian Cardiovasc Thorac Ann,* 18**,** 188-98.

SEGERS, V. F. & LEE, R. T. 2008. Stem-cell therapy for cardiac disease. *Nature,* 451**,** 937-42.

SEGERS, V. F. & LEE, R. T. 2011. Biomaterials to enhance stem cell function in the heart. *Circ Res,* 109**,** 910-22.

SEIF-NARAGHI, S. B., SINGELYN, J. M., SALVATORE, M. A., OSBORN, K. G., WANG, J. J., SAMPAT, U., KWAN, O. L., STRACHAN, G. M., WONG, J., SCHUP-MAGOFFIN, P. J., BRADEN, R. L., BARTELS, K., DEQUACH, J. A., PREUL, M., KINSEY, A. M., DEMARIA, A. N., DIB, N. & CHRISTMAN, K. L. 2013. Safety and efficacy of an injectable extracellular matrix hydrogel for treating myocardial infarction. *Sci Transl Med,* 5**,** 173ra25.

SHAPIRA, A., FEINER, R. & DVIR, T. 2016. Composite biomaterial scaffolds for c ardiac tissue engineering. *Int Mater Rev,* 61**,** 1-19.

SHEN, H., KREISEL, D. & GOLDSTEIN, D. R. 2013. Processes of sterile inflammation. *J Immunol,* 191**,** 2857-63.

SHEPHERD, D. V., SHEPHERD, J. H., GHOSE, S., KEW, S. J., CAMERON, R. E. & BEST, S. M. 2015. The process of EDC-NHS Cross-linking of reconstituted collagen fibres increases collagen fibrillar order and alignment. *APL Mater,* 3.

SILVESTRI, A., BOFFITO, M., SARTORI, S. & CIARDELLI, G. 2013. Biomimetic materials and scaffolds for myocardial tissue regeneration. *Macromol Biosci,* 13**,** 984-1019.

SOLER-BOTIJA, C., BAGO, J. R., LLUCIA-VALLDEPERAS, A., VALLES-LLUCH, A., CASTELLS-SALA, C., MARTINEZ-RAMOS, C., FERNANDEZ-MUINOS, T., CHACHQUES, J. C., PRADAS, M. M., SEMINO, C. E. & BAYES-GENIS, A. 2014. Engineered 3D bioimplants using elastomeric scaffold, self-assembling peptide hydrogel, and adipose tissue-derived progenitor cells for cardiac regeneration. *Am J Transl Res,* 6**,** 291-301.

STEINHAUSER, M. L. & LEE, R. T. 2011. Regeneration of the heart. *EMBO Mol Med,* 3**,** 701-12.

SUURONEN, E. J., KURAITIS, D. & RUEL, M. 2008. Improving cell engraftment with tissue engineering. *Semin Thorac Cardiovasc Surg,* 20**,** 110-4.

SUURONEN, E. J., ZHANG, P., KURAITIS, D., CAO, X., MELHUISH, A., MCKEE, D., LI, F., MESANA, T. G., VEINOT, J. P. & RUEL, M. 2009. An acellular matrix-bound ligand enhances the mobilization, recruitment and therapeutic effects of circulating progenitor cells in a hindlimb ischemia model. *FASEB J,* 23**,** 1447-58.

TABATA, Y., MIYAO, M., OZEKI, M. & IKADA, Y. 2000. Controlled release of vascular endothelial growth factor by use of collagen hydrogels. *J Biomater Sci Polym Ed,* 11**,** 915-30.

TALLAWI, M., ROSELLINI, E., BARBANI, N., CASCONE, M. G., RAI, R., SAINT-PIERRE, G. & BOCCACCINI, A. R. 2015. Strategies for the chemical and biological functionalization of scaffolds for cardiac tissue engineering: a review. *J R Soc Interface,* 12**,** 20150254.

USHA, R., SREERAM, K. J. & RAJARAM, A. 2012. Stabilization of collagen with EDC/NHS in the presence of L-lysine: a comprehensive study. *Colloids Surf B Biointerfaces,* 90**,** 83-90.

VILAHUR, G., JUAN-BABOT, O., PENA, E., ONATE, B., CASANI, L. & BADIMON, L. 2011. Molecular and cellular mechanisms involved in cardiac remodeling after acute myocardial infarction. *J Mol Cell Cardiol,* 50**,** 522-33.

VUNJAK-NOVAKOVIC, G., TANDON, N., GODIER, A., MAIDHOF, R., MARSANO, A., MARTENS, T. P. & RADISIC, M. 2010. Challenges in cardiac tissue engineering. *Tissue Eng Part B Rev,* 16**,** 169-87.

WANG, H., ZHOU, J., LIU, Z. & WANG, C. 2010. Injectable cardiac tissue engineering for the treatment of myocardial infarction. *J Cell Mol Med,* 14**,** 1044-55.

WANG, P. Y., YU, J., LIN, J. H. & TSAI, W. B. 2011. Modulation of alignment, elongation and contraction of cardiomyocytes through a combination of nanotopography and rigidity of substrates. *Acta Biomater,* 7**,** 3285-93.

WEI, S., CHOW, L. T., SHUM, I. O., QIN, L. & SANDERSON, J. E. 1999. Left and right ventricular collagen type I/III ratios and remodeling post-myocardial infarction. *J Card Fail,* 5**,** 117-26.

WELGUS, H. G., BURGESON, R. E., WOOTTON, J. A., MINOR, R. R., FLISZAR, C. & JEFFREY, J. J. 1985. Degradation of monomeric and fibrillar type III collagens by human skin collagenase. Kinetic constants using different animal substrates. *J Biol Chem,* 260**,** 1052-9.

WOLF, M. T., DALY, K. A., BRENNAN-PIERCE, E. P., JOHNSON, S. A., CARRUTHERS, C. A., D'AMORE, A., NAGARKAR, S. P., VELANKAR, S. S. & BADYLAK, S. F. 2012. A hydrogel derived from decellularized dermal extracellular matrix. *Biomaterials,* 33**,** 7028-38.

YANG, C., HILLAS, P. J., BAEZ, J. A., NOKELAINEN, M., BALAN, J., TANG, J., SPIRO, R. & POLAREK, J. W. 2004. The application of recombinant human collagen in tissue engineering. *BioDrugs,* 18**,** 103-19.

YANG, C. R. 2012. Enhanced physicochemical properties of collagen by using EDC/NHS-crosslinking. *Bull Mater Sci,* 35**,** 913-918.

YE, Z., ZHOU, Y., CAI, H. & TAN, W. 2011. Myocardial regeneration: Roles of stem cells and hydrogels. *Adv Drug Deliv Rev,* 63**,** 688-97.

ZHANG, J., ZHOU, A., DENG, A., YANG, Y., GAO, L., ZHONG, Z. & YANG, S. 2015a. Pore architecture and cell viability on freeze dried 3D recombinant human collagen-peptide (RHC)-chitosan scaffolds. *Mater Sci Eng C Mater Biol Appl,* 49**,** 174-82.

ZHANG, Y., THORN, S., DASILVA, J. N., LAMOUREUX, M., DEKEMP, R. A., BEANLANDS, R. S., RUEL, M. & SUURONEN, E. J. 2008. Collagen-based matrices improve the delivery of transplanted circulating progenitor cells: development and demonstration by ex vivo radionuclide cell labeling and in vivo tracking with positron-emission tomography. *Circ Cardiovasc Imaging,* 1**,** 197-204.

ZHANG, Y. S., ALEMAN, J., ARNERI, A., BERSINI, S., PIRAINO, F., SHIN, S. R., DOKMECI, M. R. & KHADEMHOSSEINI, A. 2015b. From cardiac tissue engineering to heart-on-a-chip: beating challenges. *Biomed Mater,* 10**,** 034006.